Oil & Natural Gas Technology

DOE Award No.: DE-FC26-06NT42241

Final Report

A Robust MEMS Based Multi-Component Sensor For 3D Borehole Seismic Arrays

Submitted by:
Paulsson Geophysical Services, Inc.
1215 W Lambert Rd.
Brea, CA 92821

Prepared for:
United States Department of Energy
National Energy Technology Laboratory

July 30, 2007

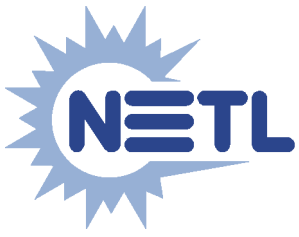

DISCLAIMER

ABSTRACT

The objective of this project was to develop, prototype and test a robust multi-component sensor that combines both Fiber Optic and MEMS technology for use in a borehole seismic array. The use such FOMEMS based sensors allows a dramatic increase in the number of sensors that can be deployed simultaneously in a borehole seismic array. Therefore, denser sampling of the seismic wave field can be afforded, which in turn allows us to efficiently and adequately sample P-wave as well as S-wave for high-resolution imaging purposes. Design, packaging and integration of the multi-component sensors and deployment system will target maximum operating temperature of 350-400 deg F and a maximum pressure of 15000-25000 psi, thus allowing operation under conditions encountered in deep gas reservoirs. This project aimed at using existing pieces of deployment technology as well as MEMS and fiber-optic technology. A sensor design and analysis study has been carried out and a laboratory prototype of an interrogator for a robust borehole seismic array system has been assembled and validated.

TABLE OF CONTENTS

EXECUTIVE SUMMARY

The aim of this project was to develop, prototype and test a robust multi-component sensor that combines both Fiber Optic and MEMS technology for use in a borehole seismic array. The use of such FOMEMS based sensors allows a dramatic increase in the number of sensors that can be deployed simultaneously in a borehole seismic array for high-resolution seismic imaging purposes. Design, packaging, material and integration of the multi-component sensors and deployment system targeted maximum operating temperature of 350-400 deg F and a maximum external pressure of 15000-25000 psi. This project tried to leverage existing pieces of deployment technology as well as MEMS and fiber-optic technology and combine them in an optimal way.

During the contract award period from October 2004 – July 2007 Paulsson Geophysical and its main subcontractor Optiphase worked on a wide range of activities from detailing specifications, designing and testing subsystems to interfacing with and selection of potential manufacturing subcontractors.

This project planned to use a two phased approach. The first phase consisted of designing and prototyping of sensor and interrogation system components, while the second phase consisted of functionality tests of assembled prototype systems in the laboratory or in the field.

Originally PGSI had planned to work with subcontractor Umachines Inc., but both parties could not come to an agreement relating the future use of intellectual property. After extended discussion Umachines retracted and in December 2005 Paulsson Geophysical, after having looked into several alternatives, proceeded with engaging Optiphase Inc as the main subcontractor to support PGSI in development of the MEMS sensor and interrogation package as well as with management of external project details and other potential subcontractors.

By year end of 2006 two events caused a change in focus of the project. One was the inability to secure a manufacturing contract with a subcontractor for construction of the MEMS sensors. The other was that Department of Energy funds for the second phase of the project became unavailable due to budget cuts. At that time with concurrence of the DOE project manager, the project was refocused to complete the basic design of the MEMS sensor without going into manufacturing; and to design, implement and test a prototype of the time and wavelength domain multiplexed fiber-optic gapped sensor interrogator by July 2007. Thus, although a MEMS sensor was not manufactured, we were able to complete some of the advanced tasks relating to the interrogation system that were originally scheduled for the second phase.

By July 2007 we were able to successfully complete the following major tasks:

- specification for a gap based fiber optic sensor

- selection of a practical sensor device design
- specification and design of sensor packaging
- test and selection of appropriate light sources
- design of an advanced interrogation system
- component tests of the interrogation system
- construction of a table top prototype assembly of the time and wavelength domain multiplexed interrogator
- completion of multi-channel performance measurements

Valuable experience has been gained in the course of this project on a variety of design, manufacturing and technical issues. This report provides a summary for the contracted activities during the project period from October 2004 through July 2007.

RESULTS AND DISCUSSION

Design and Prototyping

In the early phase of the project PGSI produced specifications of desired sensors attributes, including: sensitivity, frequency and phase distortions, dynamic range, vector fidelity, cross feed, noise floor, orientation determination, physical size, packaging, handling, and environmental rating. These guidelines were based on existing geophone specifications, as well as a existing public MEMS device specifications and performance data. The general functionality of sensor link and recording system such as fiber optic link, digitization and connectivity requirements were specified later during the interrogator development. Some of the sensor specifications will always depend on the interrogation system used and might necessitate slight changes in practice.

In cooperation with Optiphase several potential gapped sensor devices were considered, in particular a variation of the Fibresonde proprietary design was analyzed, but PGSI could not come to a contractual agreement with the holder of the intellectual property and that particular design was dropped and the following sensor approach selected.

Sensor Approach

The practical sensor approach determined by PGSI and Optiphase as the most favorable design for the MEMS sensor is a weak Fabry-Perot interferometer where one of the reflecting surfaces is a mass loaded diaphragm to enable sensitivity to acceleration. A sensor approach depicting this design type is shown in Figure 1. The weak Fabry-Perot design for this concept provides for two reflections. One, a partial reflection from the end of the fiber and a reflection from the inside surface of the diaphragm. In this embodiment, the weight of the diaphragm is the proof mass for the accelerometer. Movement of the diaphragm due to acceleration will cause a variation in the distance d, and is intended to be interferometrically detected with high resolution and accuracy. The interferometer is thereby defined by light reflecting from the fiber end (reference beam) and the light reflecting from the inner surface of the diaphragm (signal beam). Both beams propagate back to though the single mode fiber to be captured in the interrogation device.

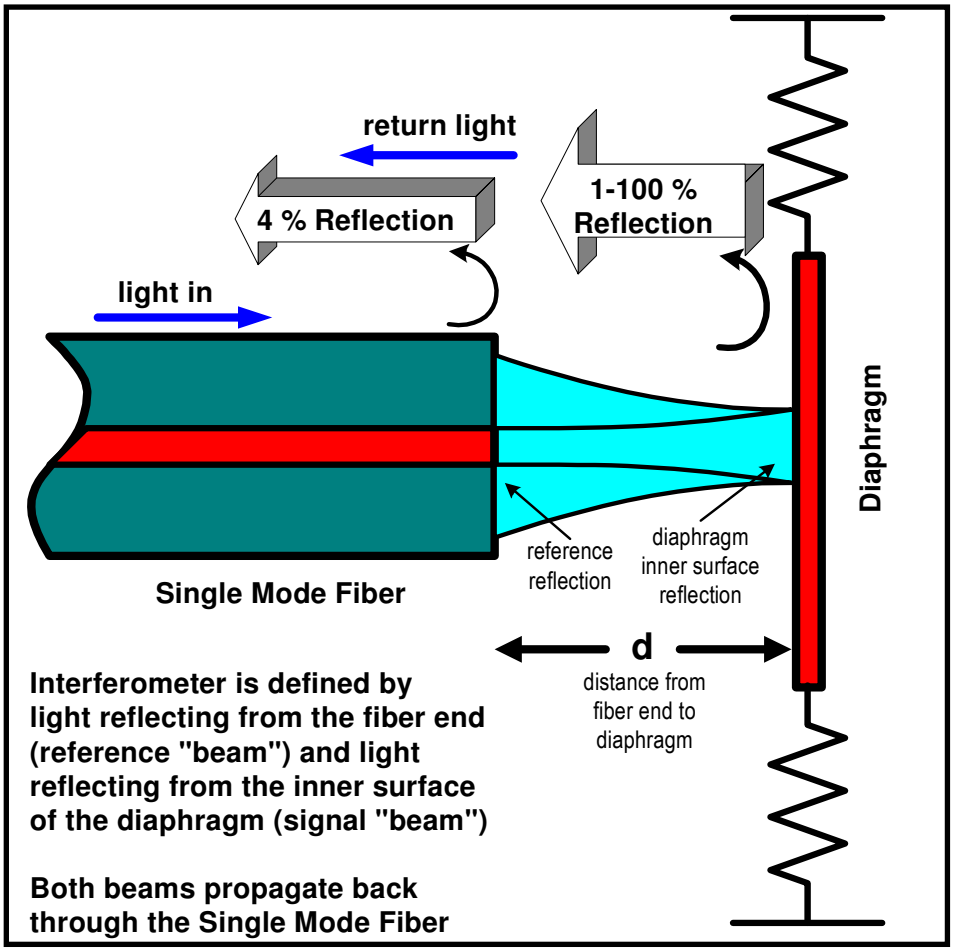

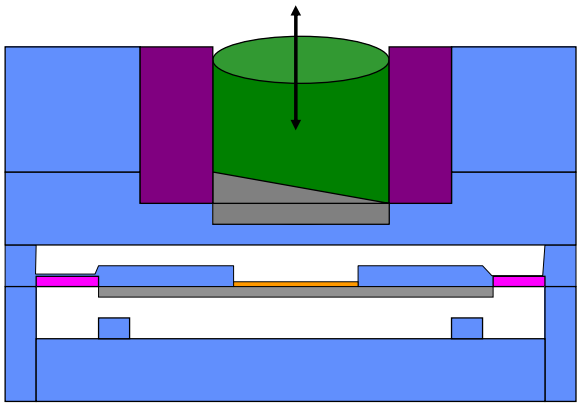

Figure 1: Weak Fabry-Perot concept (top) used in the practical MEMS sensor design (bottom).

Sensor Specifications

Table 1 shows details of the critical sensor, telemetry and interrogator specifications. The sensor type was to be characterized as a tri-axial accelerometer using MEMS optical interferometry as measurement principle while providing pure fiber-optic output and connections. A tri-axial assembly contains three orthogonally mounted single-axis sensor devices. The back reflection type can vary. However, a weak Fabry-Perot type interferometric device with a fixed optical path is most likely. The concept of the specified sensor is shown in Figure 1. The fiber-optic sensor gap was chosen such that the gap size agrees with the ITU laser frequency grid. This fact allows us to use non-specialized light sources which are readily available. Such cost considerations were early on worked into the project specifications. Since we are potentially dealing with hundreds or thousands of interrogated sensors, the ultimate commercial system cost is part of the design criteria. The sensor will be operating at nominally 1550 nm wavelength.

The insertion of a sensor should not cause a loss of more than -17 dB (optical) in the optical link. The optical fiber needs to be a bend-insensitive polyimide coated fiber which can be obtained from several manufacturers.

The signal peak acceleration should not exceed +/- 1.5 g for all spatial axes. The dynamic range is telemetry or interrogator dependent and should exceed 129 dB, with a distortion factor of less than 0.1%. The potential frequency range should be 2 Hz - 1.4 kHz. A scale factor (sensitivity) of 15 radians per G is envisioned for the interferometric interrogation.

The frequency response is device specific. However, the sensor scale factor should be stable at +/-2% at 25 C and should have a tolerance of less than +/- 5% over the working temperature range. The operating temperature is 0 to 200 C, with a storage temperature range of -40 C to +200 C.

The noise floor is related to the telemetry, interrogator and sensor scale factor related and should lie in the range of 300-500 ng/sqrt(Hz). Three-component sensor orthogonality is required to be at least 50 dB, unless the sensors have the capabilities to measure misalignment.
The sensors need to be able to withstand a shock of 1500g and the physical size is such that they can be mounted in a housing of maximum inner diameter of 1 inch.

Since the sensor will be mounted within a pressure sealed housing that is filled with air, nitrogen or argon, it will be necessary for the sensor to operate in only a low pressure environment of typically 10-50 psi. The external high pressure will be borne by the housing of the sensor assembly.

Parameter	Specification	COMMENTS
Sensor Type	Triaxial Accelerometer, MEMS Optical Interferometer with fiber optic interfaces	An assembly constitutes three accelerometers with orthogonal mount and fiber pigtails
Interferometer Type	back reflecting type Vendor Choice	Assume traditional interferometric transfer function (sinusoid), weak Fabry-Perot acceptable, fixed OPD
OPD (if "gap" sensor)	93.75 um ± 0.5 um	gap is dependent on ITU grid, gap index = 1
OPD (if other sensor)	TBD	
Interferometer OPD tolerance	± 0.5% over temperature	this is tentative spec, may revise
Optical Wavelength	C-Band, ITU grid (nominal 1550 nm)	Individual accels in triad assembly may require wavelength filters, currently TBD
Sensor Insertion Loss	not more than -17 dB (optical)	This value may change, still being analyzed.
Fiber type	Bend Insensitive, SMF, 80 um clad, polyimide coated	Fibers being considered. 1) OFS Micro-1550-21 2) Fibercore SM1550 (with polyimide coat);
Signal Range:	± 1.5 g peak, all axes	
Dynamic Range:	>129 dB	This parameter telemetry or interrogator dependent
Distortion:	≤ 0.1%	may be considered as linearity
Bandwidth:	2Hz to 1.5 kHz, 4 KHz min sample rate Possibility of DC operation if design is stable over environment	Considerations for DC coupled operation for inclination if vendor deems possible. This is desired but not required
Scale Factor (aka Sensitivity)	15 radians per G (interferometric)	below resonance subject to revision
Sensor Scale Factor Tolerance	± 2% @ 25 C ± 5% over temperature	within passband subject to revision
Resonance / Q	Vendor and Device specific	High "Q" devices may need damping to meet shock limit
Frequency Response	Vendor and Device specific	Vendor to recommend. Projections of frequency response through resonance over temperature to be provided by vendor
Storage Temperature	-40C to +200C	
Operating Temperature	0 C to 200 C	.
Noise Floor:	300-500 ng rms / sqrt(Hz)	telemetry / interrogator and sensor scale factor related
Sensor Component Orthogonality:	50 dB	possibility to relax this requirement if sensors are provided with axis misalignment values.
Shock Limit:	1500 g peak	
Physical Size:	The overall sensor assembly (including fiber pigtails) will mount inside a cylindrical pressure housing having a maximum inner diameter of 1 inch	Fibers must be able to bend with minimal loss and still maintain the 1" maximum dimensional tolerance for cylinder ID.
Operating Pressure:	10 psi – 50 psi	Will be packaged in sealed pressure can, fill gas will be air, nitrogen or argon TBD

Table 1: Sensor specification details.

Sensor Interrogation

Based on the weak Fabry-Perot sensor type selected and specified in Figure 1 and Table 1 PGSI and Optiphase designed a complex sensor interrogation system as shown conceptually in Figure 3. The interrogation system allows for time division multiplexing of signals as well as wavelength division multiplexing in order to provide the bandwidth and sampling of many channels simultaneously.

The system is modularized and it its basic form uses a four wavelength source followed by an optical pulser to implement a time division multiplex technique, an optical amplifier (EDFA) and distribution to various sensor arrays, where each module within the array contains a three axis MEMS sensor assembly. Numerous variable delay lines and line splitters apportion and balance the interrogating signal in such a way that all sensors are addressed properly. Light returning from the sensors is separated into the initial four wavelengths, where each has an interferometric phase respectively in quadrature with successive wavelengths. A four channel receiver is used to detect these quadrature components and an interrogator board performs the processing to obtain raw sensor data for each MEMS seismic sensor. A host PC is used control the interrogator and is the recipient of demodulated sensor data.

A complete sensor array comprising hundreds or thousands of levels can be composed of a set of basic array units. Each array unit can be interrogated efficiently through optimal time division and wavelength division multiplexing. The break down into basic units allows us to utilize off-the-shelf components as long as they are within the specification tolerances required. The timing monitor signal is shared for all interrogation boards, ensuring that all recordings are synchronized against the same time base. The time division pulse control is specific to each interrogation board and affects only the associated light source with a baseline of 50 ns and a width of 5-10 ns rise/fall. The repetition rate is 4 kHz to 100 kHz allowing adequate sample of the seismic recording spectrum. Signal extinction is larger than 60 dB.

The fan out, circulators and delay lines ensure that each sensor device is illuminated uniformly. Delay lines and line taps are located within the sensor assembly so that they are protected from environment and the transmission fiber has simple, clean and reliable interconnects.

Options exist to use broadband sources with external wavelengths selectors or selected wavelength band light sources. Choices are determined by cost and noise issues, but would not impact the overall design of the interrogation module.

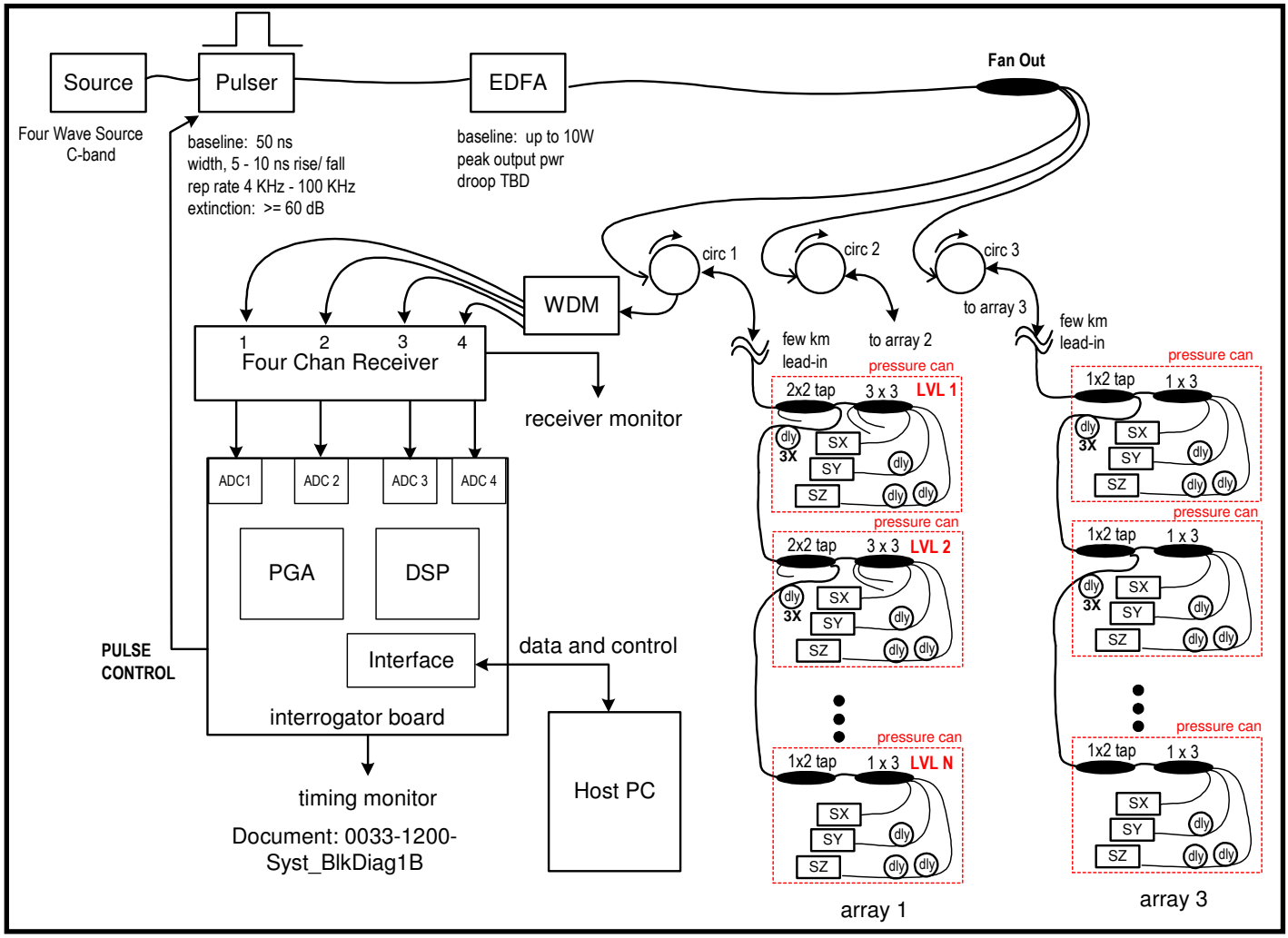

Figure 3: Interrogation and telemetry linking the sensors with the recording unit.

Conceptual Approach Selected

A conceptual approach was selected as a combination from Davidson and Mycraline, both did extensive modeling of mechanically dynamic behavior of the practical sensor implementation shown in Figure 1. However, no agreement could be reached on IP rights, thus no manufacturing was carried out.

Sensor Packaging

Based on original proprietary packaging of PGSI's sensor assembly, Optiphase and PGSI modified the design to be able to mount a MEMS sensor module. The entire design was carried out in a CAD system and aimed at having a complete set of drawings with measurement and tolerances available for PGSI's prototyping and production assembly.

We were successful at maintaining the overall form factor, such that the current PGSI clamped borehole deployment system could be used without further modification. This makes a potential field trial possible where traditional geophone based sensors and the fiber-optice MEMS sensor can be deployed simultaneously in the same borehole and seismic waves emanating from the same source are captured into the traditional as well as in the fiber-optic sensor array. In situ, clamping and environmental variations are thus minimized and direct comparison is possible. In this manner a hybrid sensor system could be manufactured if a practical reason should require it.

In the following we show some example views detailing the individual sensor mount and their relation to protective housing.

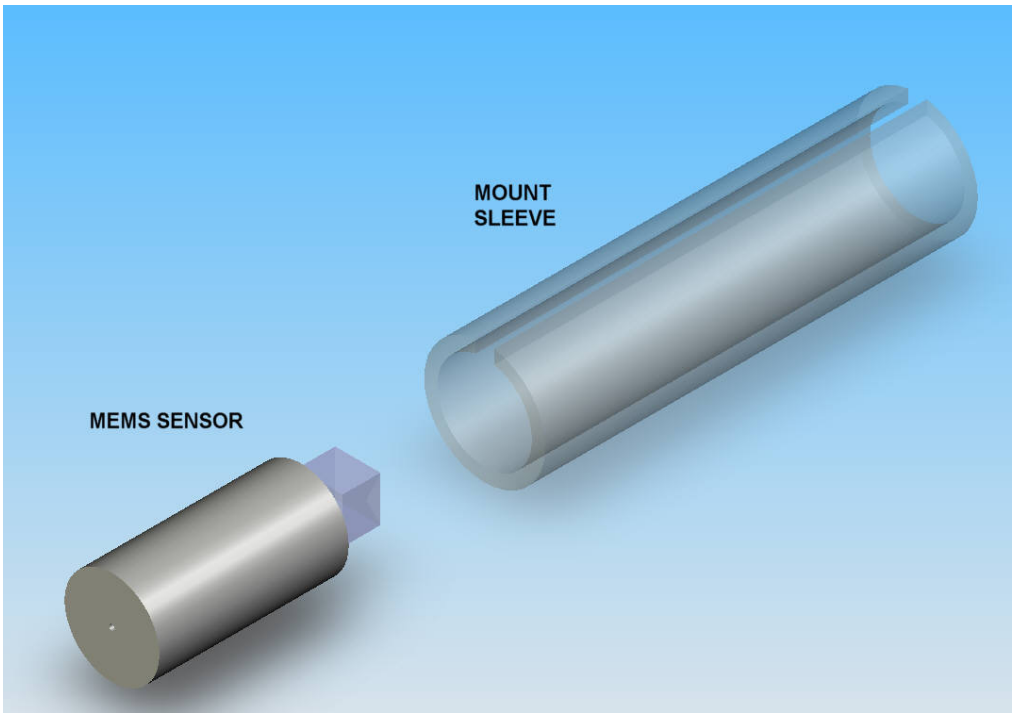

Figure 4: MEMS sensor and individual alignment sleeve .

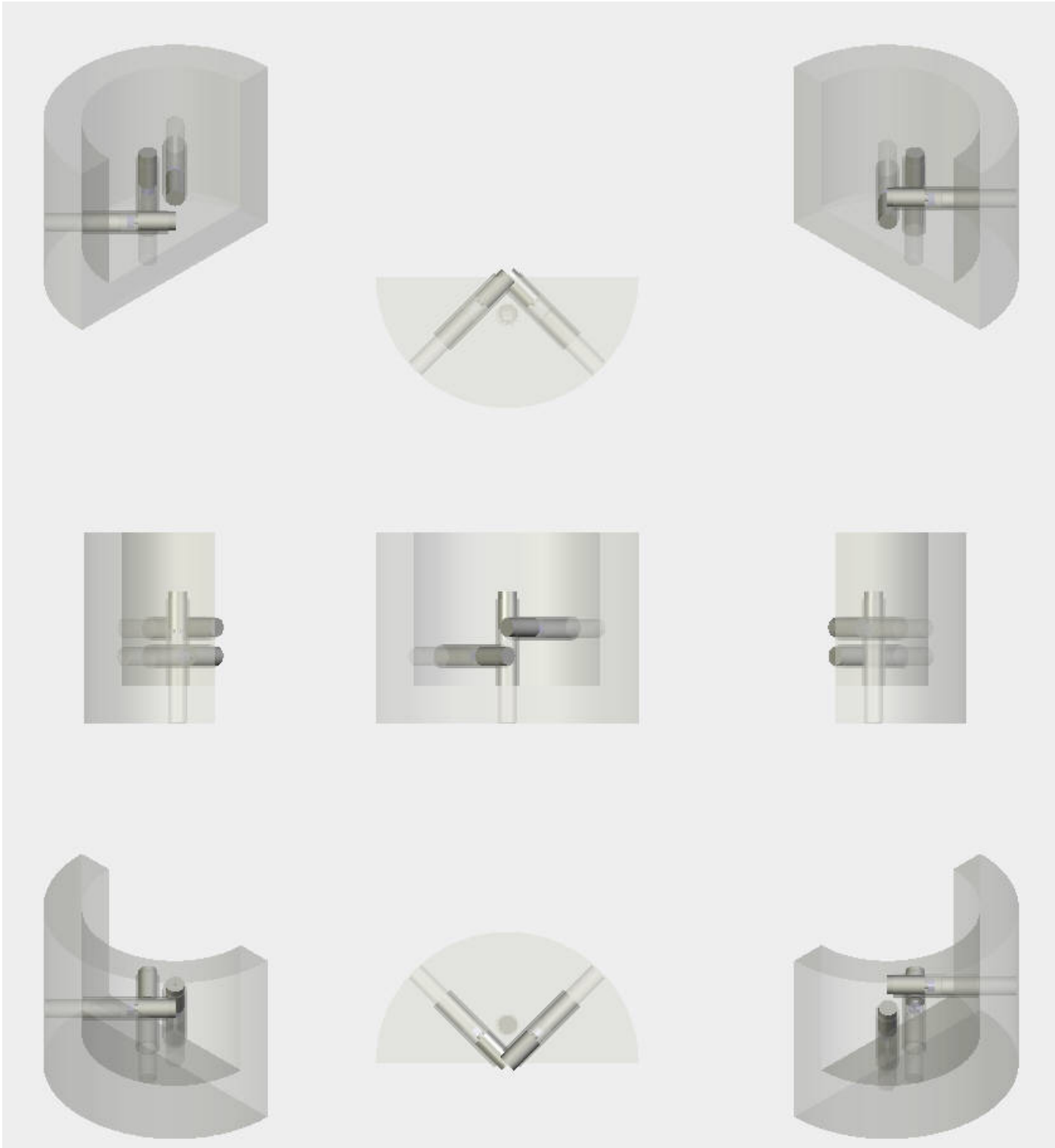

Figure 5: Orthogonal mounting of the sensor triad

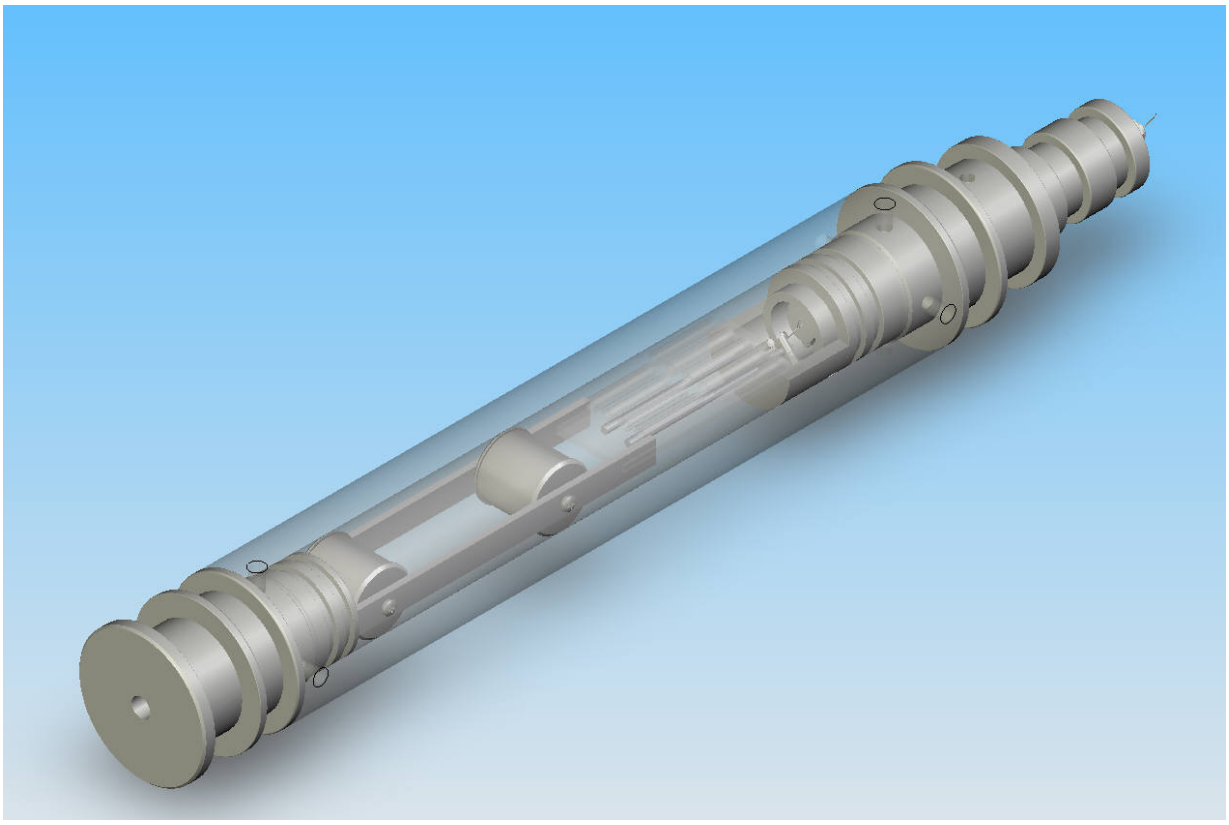

Figure 6: Assembly of the sensor package in the housing.

Interrogator Development

Besides the MEMS sensor conceptual design and packaging, the interrogator development was the main focus of the remaining activities. Some of the tasks that were originally scheduled for Phase 2 were accelerated and included into Phase 1 activities.

Since the interrogator is the backbone of the sensing system great care was taken to design the system and its component, as well as to test and select subcomponents.
As shown in Figure 3 the complete interrogator consists of several critical components. Optiphase followed a methodical design and test procedure for each of the components.
The following sections report on various subcomponents of the interrogator, the integrated interrogator and laboratory test results. In this part of the report we summarize only the main observations and conclusions from Optiphase's activity report.

Optical Source

The optical source is a critical component driving the interrogator. The basic sensing approach is shown in Figure 7.

A four wavelength optical source sends light to the MEMS sensor which is essentially a Fabry-Perot device configured for weak reflections to form a two beam interferometer. The light signals are reflected from a mass loaded diaphragm that is sensitive to seismic vibration (acceleration) signals. The four wavelengths are specifically selected to match the path mismatch of the Fabry-Perot device. We are considering gaps between 100 to 200 um such that each wavelength returns with an optical phase of pi/2 (quadrature) with respect to each other. The reflected light signals then enter the circulator and reach the wavelength division multiplexer. The receiver and demodulator conditions and processes the signals' phase shifts and outputs them digitally. This overall approach is designed for multi-channel time division multiplexing interrogation of an array of MEMS sensors, but is shown here as a single channel sensor for clarity.

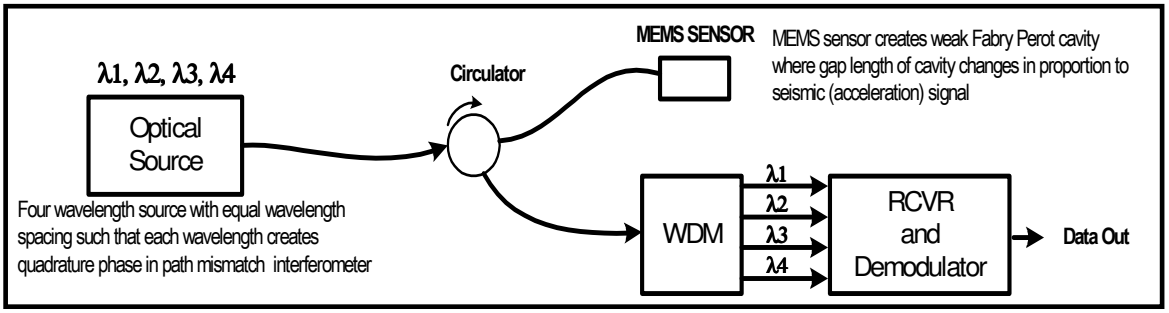

Figure7. General diagram for sensing and interrogation approach is shown for single sensor

Since it is critical to find the best approach for the multi-wave-length optical source, we configured and tested two types of multi-wave-length optical sources; both arrangements are contrasted in Figure 8.

In Figure 8, approach 1, we use a broadband source followed by a telecommunications (telco) WDM device which separates the light out into four different wavelengths. These WDM devices use narrowband optical filters set to precise wavelengths and separate them out to four different fibers. A separate WDM device is used to put these narrowband devices back in the same fiber.

The second approach is more traditional where four separate lasers are used and multiplexed together with a WDM.

The reason for considering the broadband approach is, that these type of sources are much less coherent than distributed feed-back (DFB) devices and errors from multiple scattering and coherent Rayleigh backscatter would be non-existent.

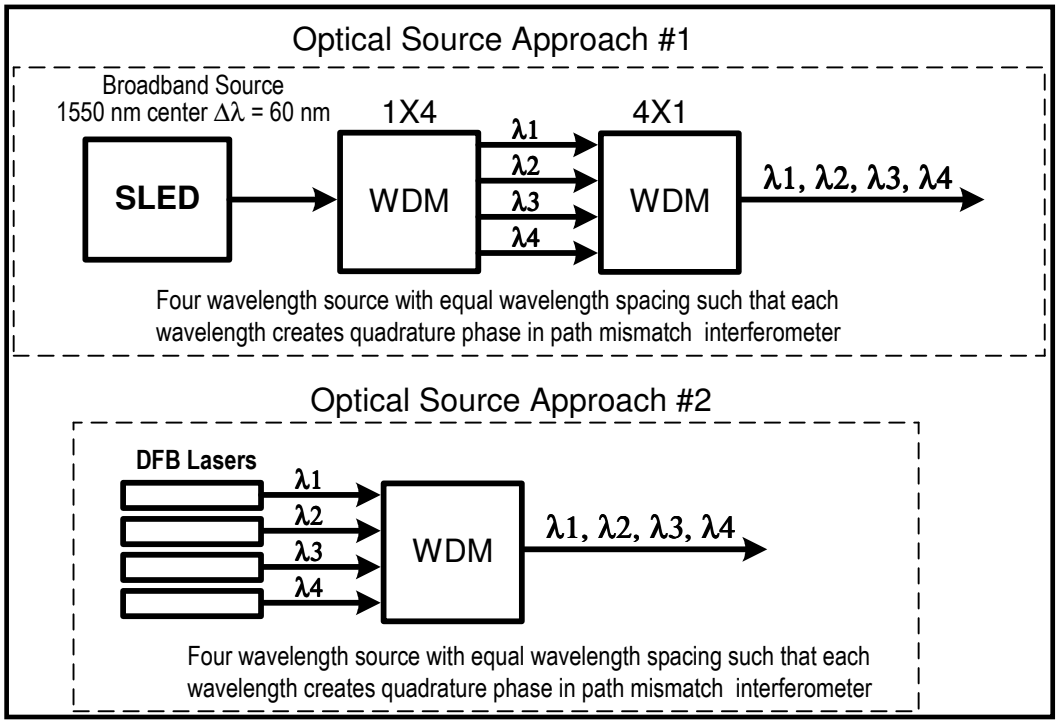

Figure 8. Two source configurations considered. Approach 1 (top) uses a broadband source which is sliced up into four wavelengths. Approach 2 (bottom) uses four separate DFB lasers.

Tests Conducted

A Weak Fabry-Perot active interferometer was constructed to test both source types. These tests were conducted to determine both Phase Noise and Relative Intensity Noise of both source types. Phase Noise and Relative Intensity have a first order impact on the performance of the interferometric interrogation. The testing was only performed at one wavelength, since that is all that is needed for such performance testing. The three different test sources were:

1. Broadband source (1550 nm) with 200 GHZ OADM filter (1200 pm pass band)
2. Broadband source (1550 nm) with 100 GHZ OADM filter (600 pm pass band)
3. DFB (distributed feed-back lasers, telecommunications type at 1550 nm)

The first broadband source with a 1200 pm pass band is measured in Figure 9. It confirms that there is enough coherence for a 200 um gap sensor.

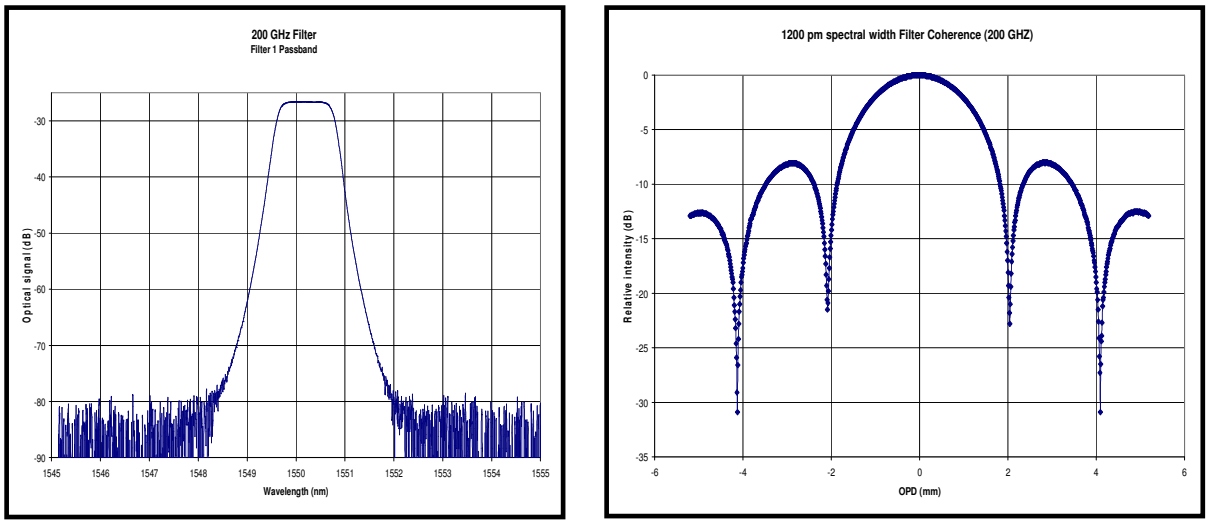

Figure 9: Spectrum and coherence function as measured in the broadband source with 1200 pm passband (100 GHz OADM).

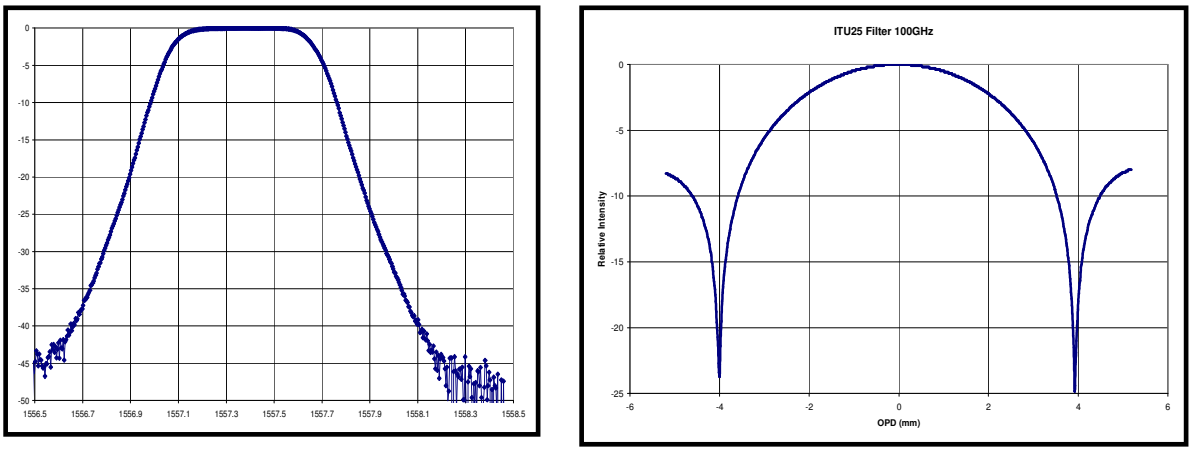

Figure 10: Spectrum and coherence function measured in the broadband source with 600 pm passband (100GHz OADM).

The second broadband source with 600 pm pass band is measured in Figure 10. It also proves to have a wide enough coherence for a 200 um gap sensor.

The phase noise and relative intensity noise measurements were performed with a 94 um gap sensor. The total optical path distance is 188 um and demodulation uses 39 kHz. Figure 11 shows the results for all three source types. The DFB performs with extremely low phase noise. All relative intensity tests were performed with a 20 uW quiescent level.

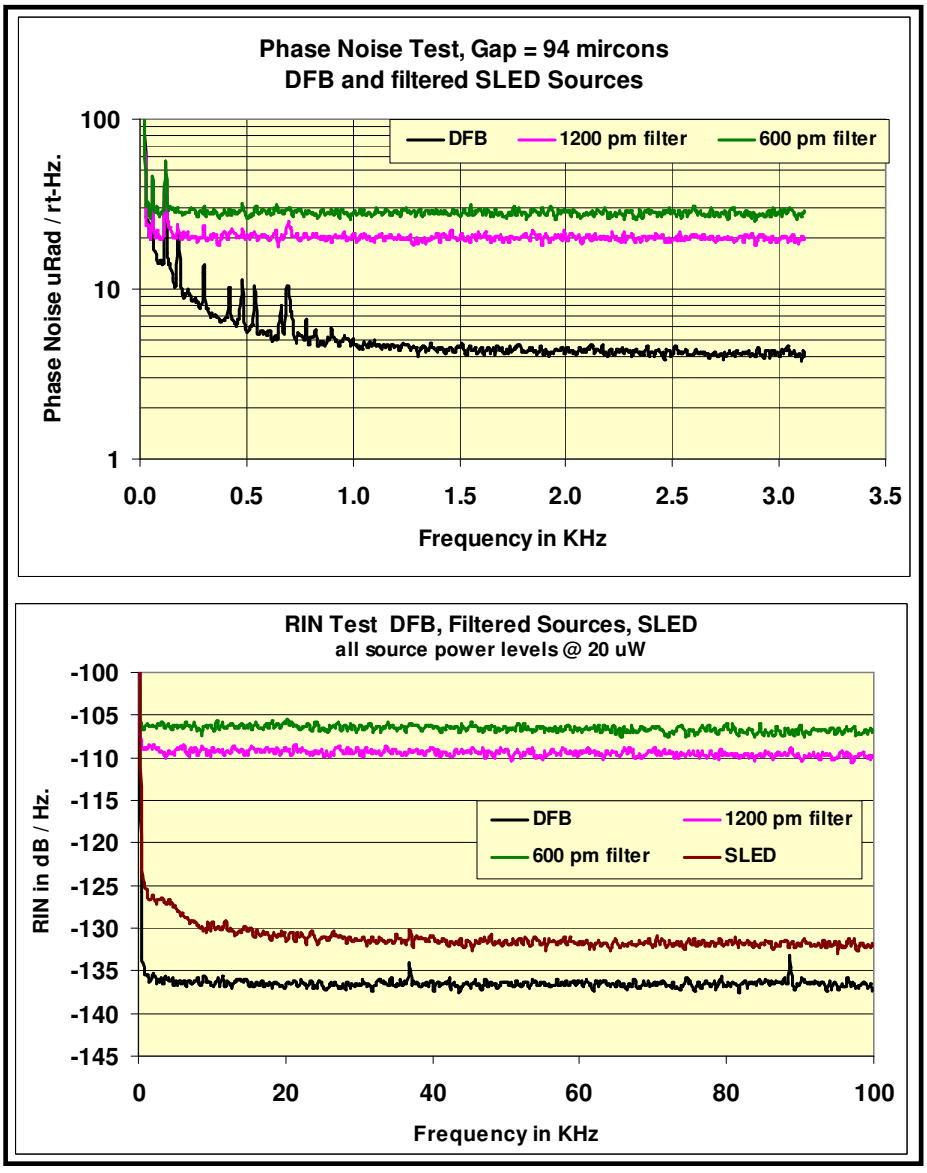

Figure 11: Phase noise (top) and relative intensity noise performance (bottom) various sources.

The phase noise for the filtered source is slightly higher than anticipated. The narrow line source (600 pm filter) than the wider line source (1200 pm filter). We estimate that this likely due to the quantized nature of wavelengths which make up each source. This

consideration is somewhat validated by observing the Relative Intensity Noise (RIN) in Figure 10. The narrow filter source (600 pm) has a higher noise floor than the broader (1200 pm) source.

Design Conclusions

The filtered source experiment provides a phase noise at 1200 pm which is roughly 2 times higher than what is ideally desirable. However, it is still useable. The 600 pm source exhibits 3 times higher noise than is desirable and also provides half of the light output as compared to the 1200 pm source. Thus, the 600 pm source was not considered for future use.

It was determined that evaluations of the integrated system would only use the following:

1. Four wave Source with SLED and 200 GHZ OADM WDMs
2. Four wave source with DFB's

The reason for still considering both is that under given circumstances it is expected that the DFB system will provide numerous errors due to its high coherence and the SLED approach may actually outperform it due to its low coherence protection.

Broadband Source With Spectral Slices

The optical source approach 1, shown in Figure 8, uses a broadband optical source with a well behaved spectral characteristic. Per design, the wavelengths and other parameters have been chosen as:

ITU 27	1555.75 nm	P out:	10 mW max	tunability: +/- 1 nm
ITU 31	1552.52 nm	P out:	10 mW max	tunability: +/- 1 nm
ITU 35	1549.32 nm	P out:	10 mW max	tunability: +/- 1 nm
ITU 39	1546.12 nm	P out:	10 mW max	tunability: +/- 1 nm

The lasers were manufactured by CyOptics Inc. (Breingsville, PA). They are all single longitudinal line, multi-quantum-well (MQW), distributed-feedback (DFB) lasers, packaged in industry standard 14 pin butterfly packages with PM fiber pigtails. They have integrated temperature controllers for wavelength control or stability (constant temperature) and have an integrated optical isolator. The drive circuitry was implemented for these lasers to both control the temperature and provide a low noise constant current source, which is adjustable to set output power levels. These lasers are capable of output powers in excess of 10 mW.

The four lasers and associated drive circuitry and WDM were configured in an enclosure as depicted in Figure 8 (source approach #2). This enclosure uses standard wall power.

Figure 13 shows the front panel of the enclosure. There are controls for adjusting the output optical power of each laser and an optical output for the combined wavelengths through the internal WDM.

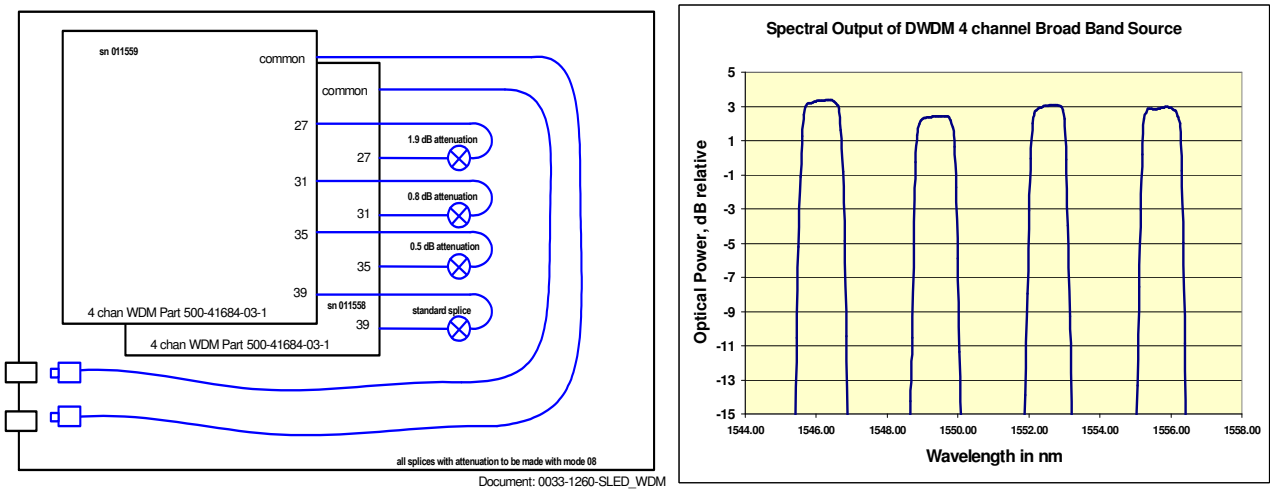

Figure 12: Wavelength division multiplexing arrangement (left) to deposit four wavelengths onto a single fiber assuming a broadband input source (Exalos model EXS 1520-2111 SLED@1550nm) and its measured output spectrum (right).

Figure 13: Completely assembled four channel DFB laser module.

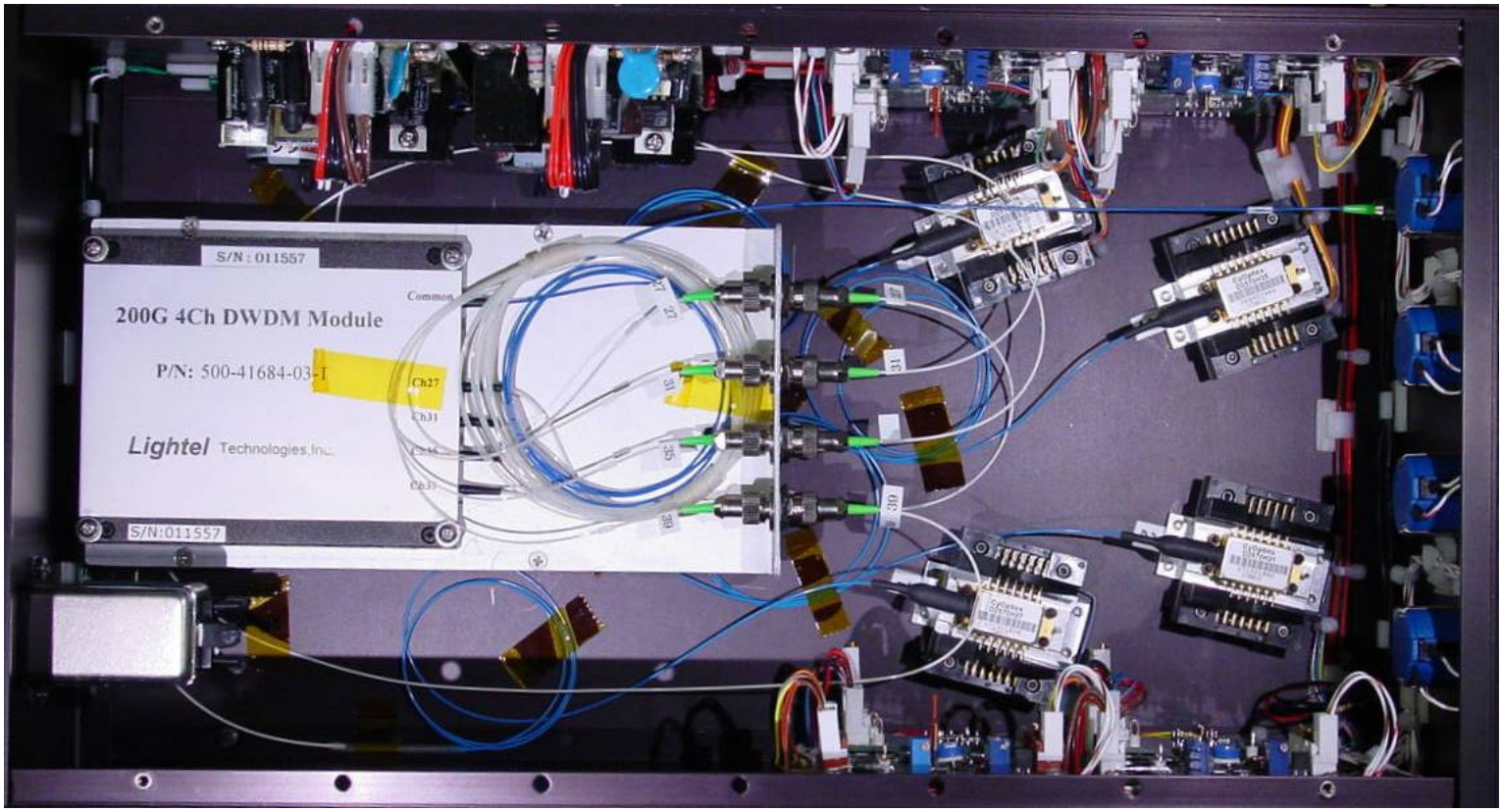

Figure 14 shows the internal arrangement of the elements of the four channel laser within the chassis shown in Figure 13. Front panel is pointing to the right.

We constructed this source assembly from its individual components in a compact chassis. It consists mainly of:

1. The four lasers. These are the devices mounted on the bottom of the chassis with heat sink mounts and wiring harnesses.

2. Laser Diode Drivers. These include modules for setting temperature of laser and drive current. These modules are located on the side walls of the instrument close to the lasers. Temperature is controlled by trip-pots on the boards. Drive current and output power is controlled from the front panel dial pots.

3. WDM module. The wave-length division multiplexing module takes light from each of the laser and multiplexes it onto one fiber. Output fiber is sent to the front panel.

Multi-wavelength Source SOA Pulser tests

A critical component of the interrogation system is the module that allows pulsing of the laser source to achieve the time domain division multiplexing. To evaluate the performance a test setup was used as shown in Figure 15.

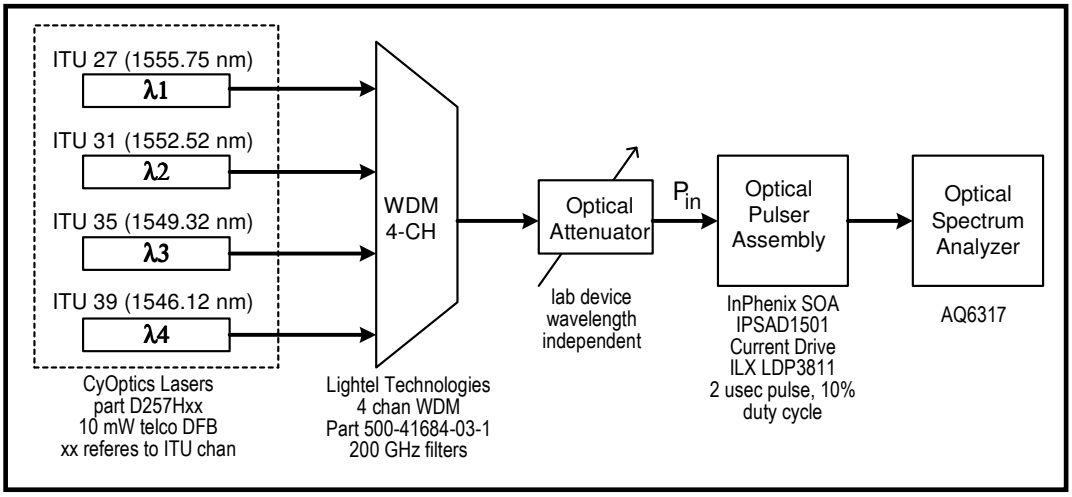

Figure 15: Pulser test layout for analyzing the spectrum of the pulsed multi-wavelength source.

The basic configuration involves four channel laser muxed with WDM, which is then attenuated so that input power is about 4 mW. This signal is then subjected to the optical pulser assembly, with 2 uW pulses on 10% duty cycle. Details of elements used are defined in the diagram in Figure 15. Pulse width and repetition rate are not at system width and design data rates, but the wider pulse and high repetition rate was useful to make accurate measurements with the optical spectrum analyzer. The optical spectrum analyzer (OSA) resolution filter for all tests was set to 0.1 nm. For all plots shown, 10 dB is equal to an intensity change of a factor of 10.

Figure 16 and 17 show several typical spectrum plots. One set of test is pulsed, see Figure 16. Another set of tests is run up to various stages of interrogation system, see Figure 17. The spectrum data show small level of mixing, and based on these tests, we concluded that adverse effects introduced by the SOA for a multi-wavelength source are minimal.

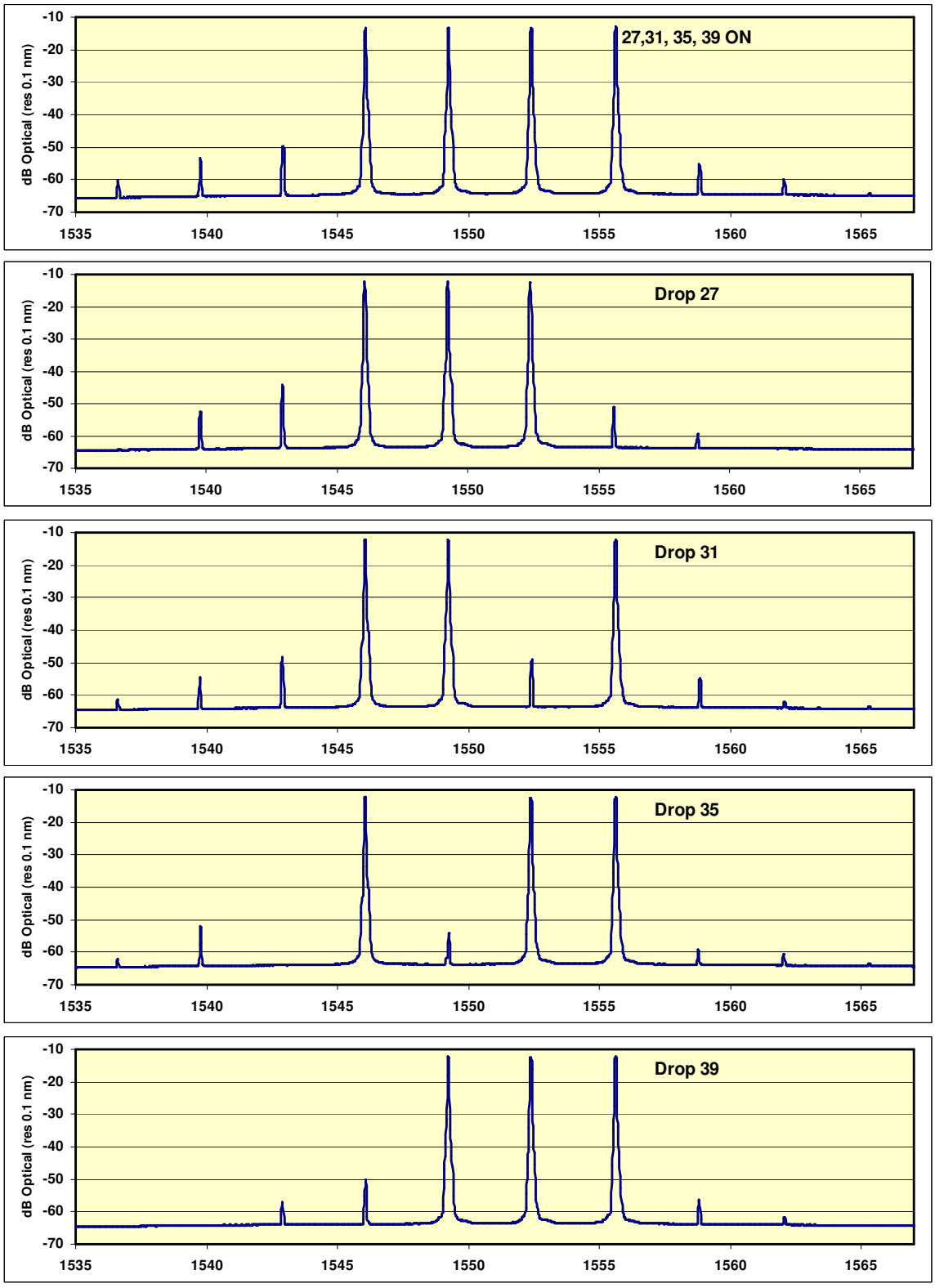

Figure 16: Output spectrum after pulser applied to a variety of input signal combinations.

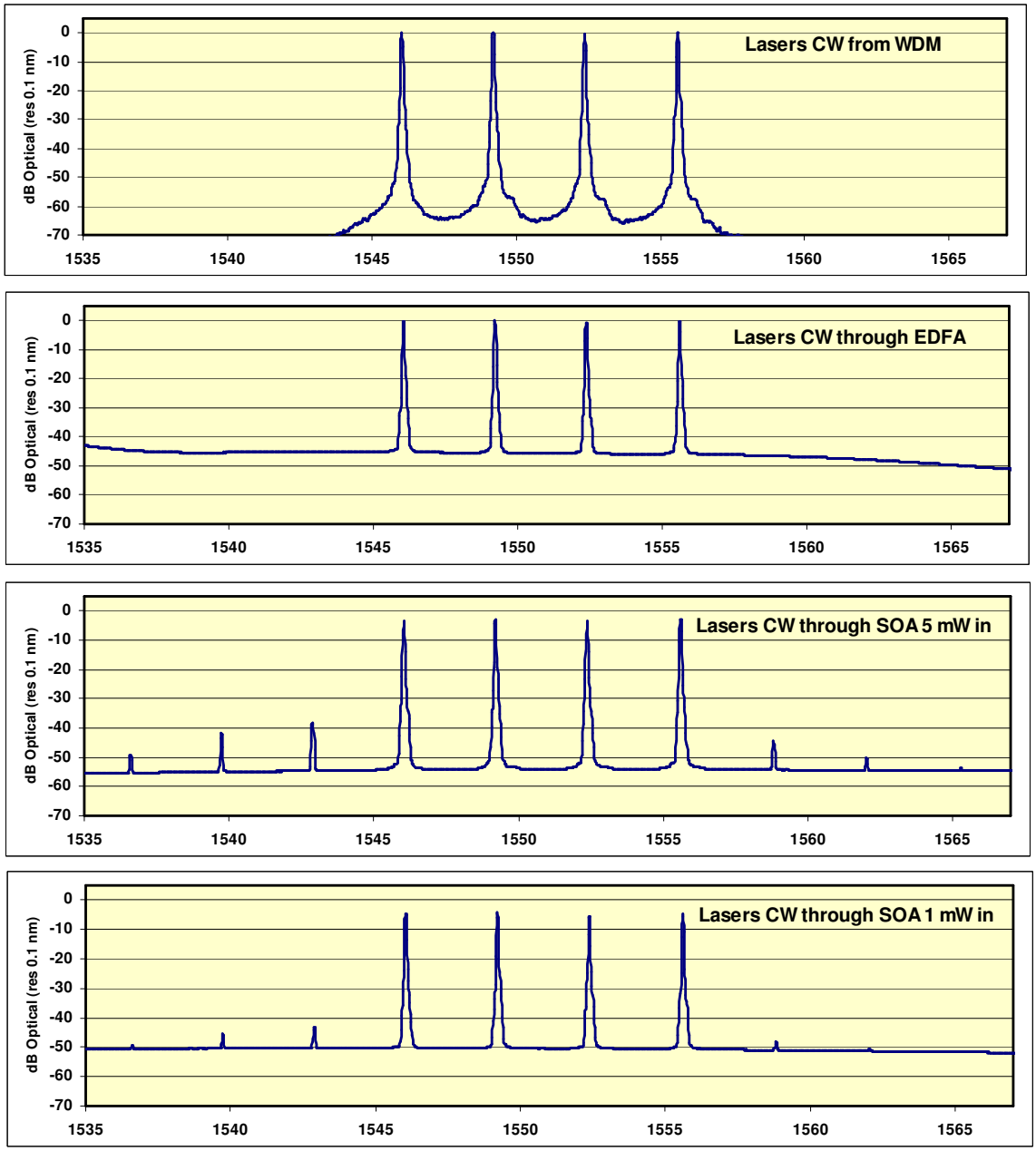

Figure 17: Output spectrum for four laser combined input at various stages through the system.

Broadband SLED / WDM Source

For completeness the broadband SLED source beam was split into four separate wavelengths in the wavelength division multiplexer and reconstituted before the light entered the optical pulser.

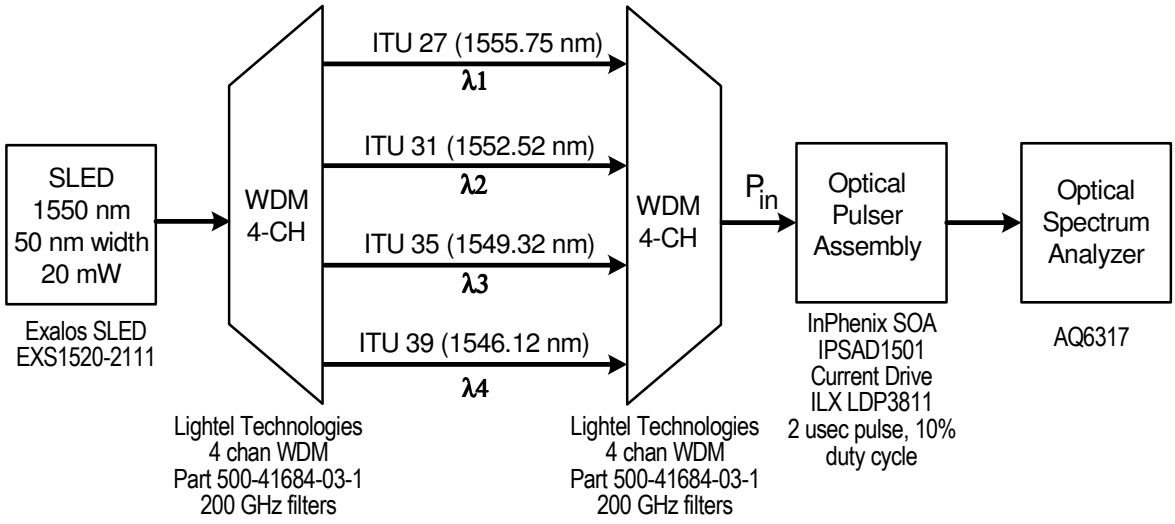

Figure 19: Test setup for the broadband source being split, reconstituted and pulsed.

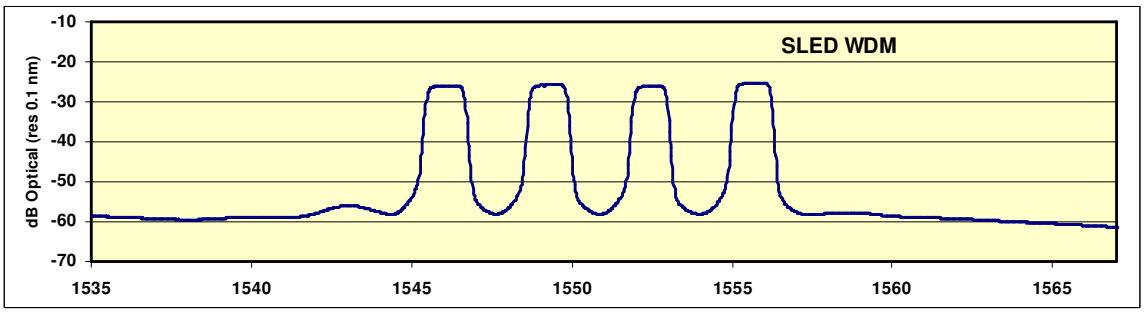

Figure 20: Output spectrum of the pulsed broadband SLED/WDM source.

Simulated Sensors and Telemetry

In order to test the reliability performance of the telemetry system a prototype system was constructed that contained six channels with sensor mockups that allowed the controlled displacement for each sensor channel. This test bed implements the optical telemetry components as designed in the block diagram for the interrogator, shown in Figure 3.
It is suitable for testing several different types of light sources, the SLED with wavelength division multiplexing as well the Laser Diode with wavelength division multiplexing. The sensors in this test configuration are simulated to be weak Fabry-Perot sensors by using the fiber end for the first reflector and piezo-electric actuated mirrors for simulating the diaphragm displacement in a precisely controlled manner.

The optical telemetry test bed was constructed to provide six sensors, each having a sufficient delay for a typical 50 ns pulse of light. This is identical to the telemetry present within the housing of a three-component sensor package. Figure 21 shows the specific layout for the six channels (2 three-component sensors).

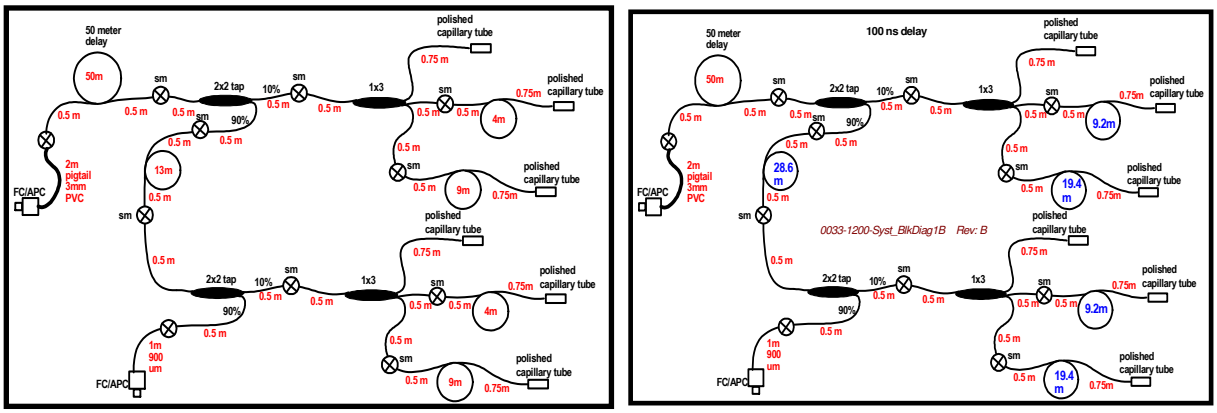

Figure 21: Optical telemetry for six channels, left for 50ns light pulse and right for 100 ns light pulse.

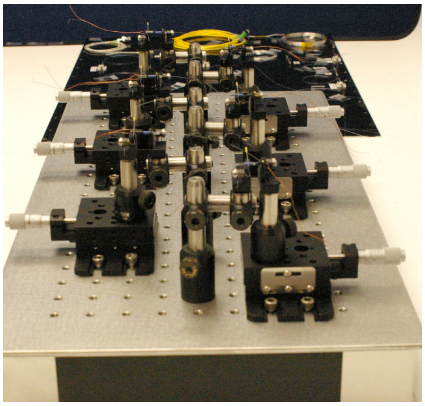

Figure 22: Table top test bed assembly for interrogator.

With the project status changing in early 2007 to only perform simulation of the MEMS sensors to test the integrated system, we decided to implement some cost savings measures related to the digitizer hardware and the optical telemetry. Such changes would have no impact on the evaluation of the interrogation technology.

For the digitizer, we reduced the input sample rate to 10 MHz (Strategic Test UF2-3131) rather than the previously selected 25 MHz (substantially higher cost UF2-3132) and selected the corresponding change to the optical telemetry architecture to allow for 100 ns pulses to accommodate the 10 MHz sample rate, as shown in Figure 21. Thus, the interrogator system used the UF2-3131 digitizer rather than the UF2-3132 digitizer.

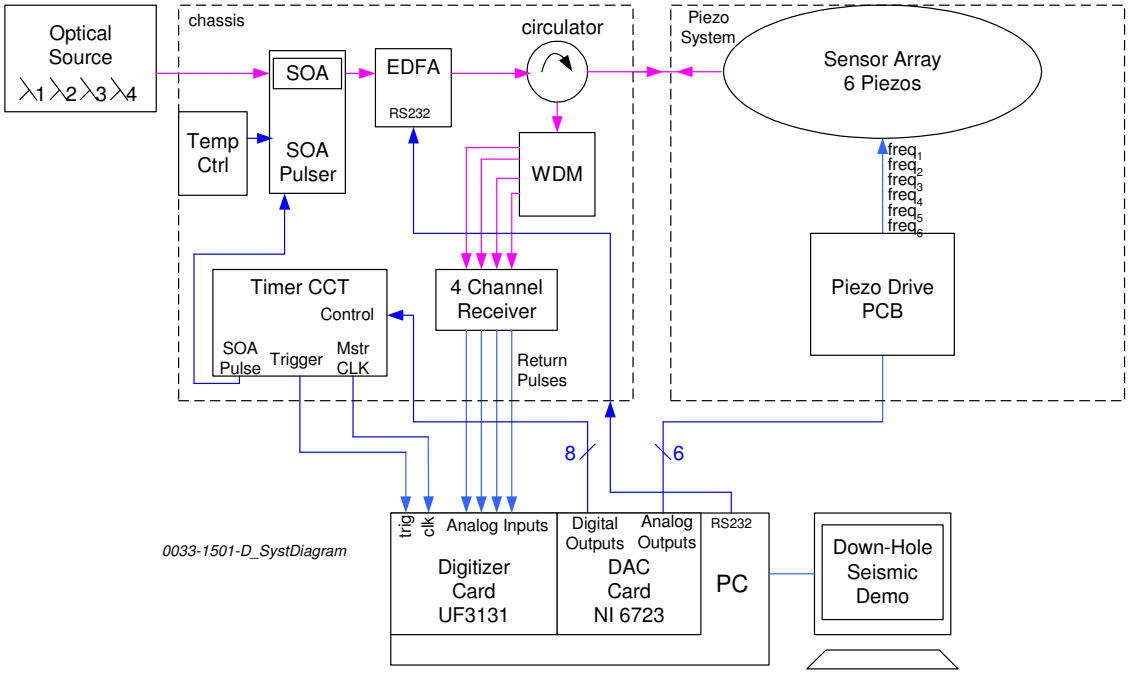

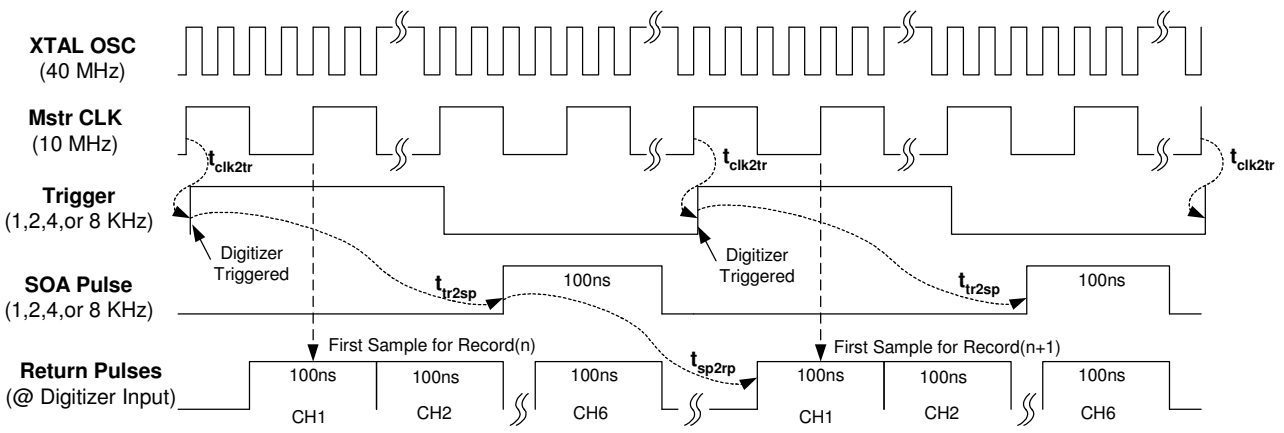

XTAL OSC is the Timer CCT board's internal 40MHz Crystal Oscillator.

Mst CLK is the Timer CCT board's 10MHz Clock Output used to drive the Digitizer Card's Clock Input.

Trigger is the Timer CCT board's Trigger output used to drive the Digitizer Card's Trigger Input.
Its frequency is **M * Mstr CLK / (10000),** where **M** is 1 to 4 yielding a Trigger Rep Rate of 1KHz, 2KHz, 4KHz, 8KHz and is set by DIP switches on the Timer CCT board.

SOA Pulse is the Timer CCT board's SOA Pulse output used to drive the SOA Pulser. It is 100ns wide and delayed (t_{tr2sp}) from **Trigger** rising edge by **(N_{course} *256 +N_{fine}) / XTAL OSC ,** where N_{course} is 1 to 256 and is set by DIP switches on the Timer CCT board, and N_{fine} is set by the **Control** input. This provides a delay (t_{tr2sp}) of 25ns to 1.6834ms

Return Pulses are the optical return pulses converted into electrical pulses and sampled at the Digitizer. The first return pulse (CH1) is delayed (t_{sp2rp}) roughly 600ns from the **SOA Pulse**. The remaining pulses for CH2 through CH6 are 100ns apart. These delays are fixed and system dependant.

Figure 23: Key elements and timing diagram for the interrogation system.

Interrogator System Element Choices And Assembly

The use of existing Optiphase components, newly designed Optiphase components, and off-the-shelf (COTS) external components were investigated. For the test bed demonstration unit, it was determined that existing Optiphase SOA Pulser (Optiphase, Inc. part 0016-2050)and Timer PCB (Optiphase, Inc. part 0032-3242) would be suitable; however, the Optiphase Timer PCB's PLD needed its code modified. These two circuit boards (PCBs) along with EDFA, circulator, WDM fit into a single chassis. Also part of this single chassis was a custom, 4-channel, Wideband Receiver PCB which is a design created for this activity and is discussed in a subsequent section. It was also determined that the optical sources will reside in their own chassis, given that two separate source types would be evaluated.

COTS PC-based Digitizer and digital-analog converter (DAC) cards were investigated. A significant requirement of the Digitizer card was a multi-record feature where a record is acquired each time an external trigger occurs, and that this happens without software intervention or re-arming. The Strategist Test UF3131 Digitizer card together with associated cabling was selected. For the DAC card, a significant requirement was the ability to drive eight piezo-electric actuators at 20Volts. For the DAC card, the National Instruments NI-6723 card was selected, along with cabling and breakout boxes. A computer (PC) was selected based on the requirement of having sufficient PCI slots. The Dell Precision 390 found suitable. The off-the-shelf PC was configured with ADC and DAC drive cards, initialized, updated, and appropriate software and card specific software drivers were installed.

The Optiphase SOA Pulser was assembled and tested. The Optiphase Timer PCB was already assembled, but its PLD code needed to be modified. Other components were purchased externally.

Four-Channel Wide-band Receiver Design Test and Assembly

The design of the wide–band receiver, shown in Figure 24, consists of a photodiode (InGaAs PIN device, nominally 100 um active area), a trans-impedance amplifier comprised of a low noise FET input, high speed operational amplifier, a Voltage controlled gain post amplifier (dc coupled), followed by a bias network to provide for bipolar voltage signals. The optical receivers, when dc coupled are “one-sided” with respect to voltage levels. Bipolar voltages are typically preferred for post digitizing systems, so the bias network takes care of that. Since we are working with high frequencies (minimally 25 MHz), we need a high speed line driver capable of driving into 50 ohm transmission lines to the Analog to Digital Converter (ADC).

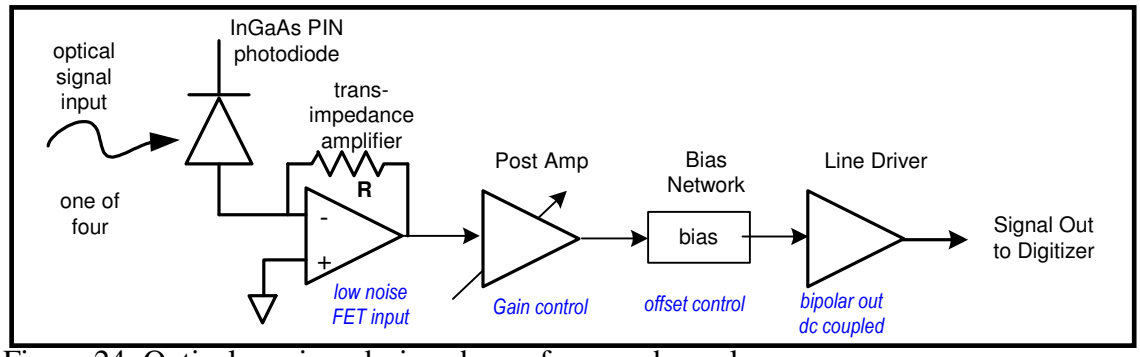

Figure 24: Optical receiver design shown for one channel.

This design investigation consisted two parts. First understanding the issues related to wideband photo detector design, and secondly, capturing those issues into a design spreadsheet for further investigation. The goal was to examine different amplifiers and all noise components, then determine achievable trans-impedance gains, bandwidths, and signal to noise ratios. The following is a summary of results using op amp OPA847 as the trans-impedance amplifier for assumed optical return levels of 10, 25, and 50 micro-amps of photo conversion current. At 1550 nm, this assumed nominally 10, 25 and 50 micro-Watts of return power for each of the sensors in the array.

TIA Gain (ohm)	BW (MHz)	Diode Signal Current = 10uA			Diode Signal Current = 25uA			Diode Signal Current = 50uA		
		SNR (dB)	SNR (bits)	Amplitude (V)	SNR (dB)	SNR (bits)	Amplitude (V)	SNR (dB)	SNR (bits)	Amplitude (V)
12000	74	46.0	7.6	**0.12**	53.1	8.8	**0.3**	57.9	9.6	**0.6**
9100	97	44.5	7.4	**0.091**	51.7	8.6	**0.2275**	56.6	9.4	**0.455**

This design considered all the possible noise sources for the process and was implemented to optimize the overall signal to noise ratio of the receiver process. Noise sources considered were:

- Dark Current from InGaAs PIN
- Shot noise from the three return optical signal levels
- Post Amp (gain control) input noise
- Op-Amp Noise Voltage (input and output referred to input)
- Op-Amp Noise current (caused by *shot noise of* offset current)
- Op-Amp and Photodiode capacitance terms which contribute to high frequency noise gain
- Thermal (Johnson) noise created by the feedback or trans-impedance resistor

Other parameters considered related to

- Low Offset Voltage (and variations over environment)
- Sufficient closed loop bandwidth to reduce ringing (or constrain damping)
- Op-Amp gain bandwidth product
- Long term objective to operate with minimally 50 MHz bandwidth (for shorter target pulse widths).

Based on all parameters analyzed, we selected the best candidate op-amp and best suited trans-impedance resistance. Thus, the design selections were:

- Texas Instruments OPA 847 (selected over OPA 846, OPA656, OPA846, OPA657)
- Trans Impedance = 12 Kohm

Detailed diagrams and documentation of the wide-band receiver can be found in the Appendix, which details Optiphase's activity report.

Piezo-Electric Driver Circuit

Following the block diagram in Figure 23, there was a need to have a Piezo Drive buffer circuit as the drive capability (current) of the DAC card (NI-6723) wasn't sufficient to drive the Piezo simulation elements in the system. The gain block for a single piezo drive involves differential drive opposing voltage buffers as shown from the excerpt of the schematic for this circuit (Figure 25, left).

Figure 25 (right) shows the wiring diagram from the DAC card (NI-6723 68 pin connector) to the piezo elements in the interferometer.

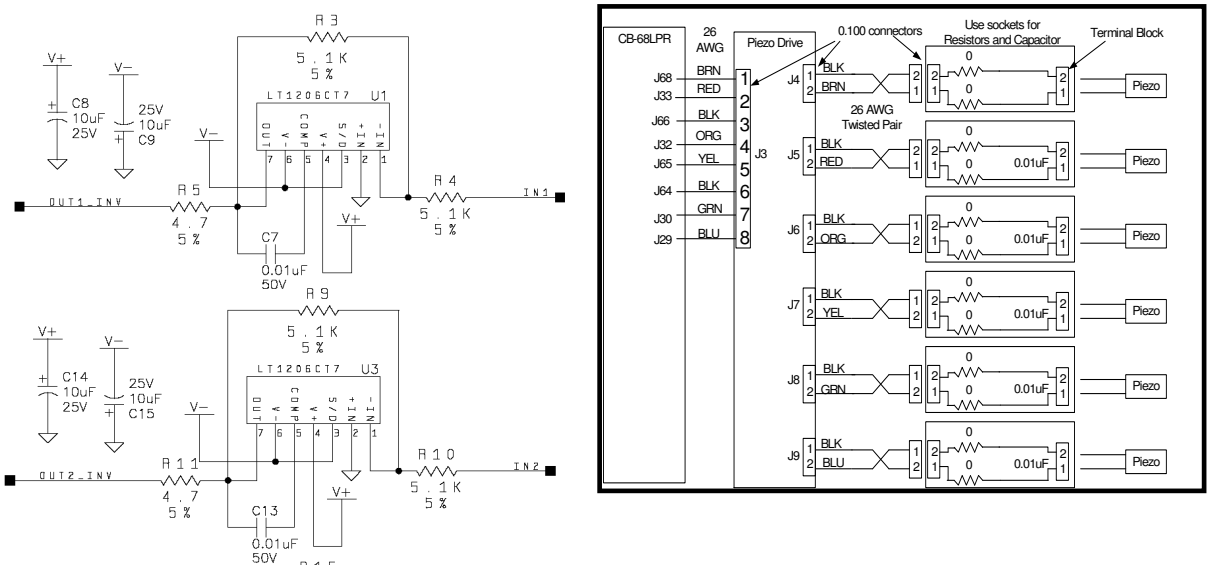

Figure 25: Piezo-electric drive gain block diagram (left) and wiring diagram (right).

The Piezo Driver Software was developed with capabilities to drive 1 to 6 Piezos with sinusoids up to +/-20V and up to 10kHz. The number of Piezos, the amplitudes, and the frequencies are set via a user interface. The Piezos can be driven continuously until the user stops or for a fixed time duration. This process is accomplished using on-board memory only, which frees up the PCI bus for Digitizer (A/D) Card activity.

Additionally, the Piezo Driver Software can accept a user data text file (txt or rtf) which contains UPDATE RATE and DATA for driving 1 to 6 Piezo Channels. If the user date file contains 1023 data points or less, on-board memory will be used, which frees up the PCI bus for Digitizer (A/D) Card activity. Examples of data files have been created and documented. For the interrogator performance tests the Piezos can be driven continuously while repeating the user data or for a fixed time duration.

Interferometric Demodulation of the Gap Sensor

This section presents the fundamental signal processing relationships to extract the optical phase measurement from the gap (MEMS) interferometers which constitute the seismic sensors for the downhole seismic recording application. The software was developed (in LabView environment) to implement this process approach.

Gap Sensor

A simple gap sensor is shown below as consisting of a first fixed partial reflector and a second reflector that is sensitive to external effects **ΔL**. Light is directed at the first reflector and a portion comes back as the optical power **P**, while part is transmitted and reflected from the second surface and returns as the optical power **Q**.

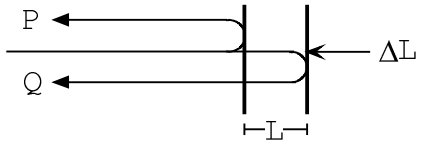

$$\theta = \frac{2\pi n}{\lambda} \cdot 2\Delta L$$

An optical detector sees the combined optical power from the interference of the light **P** with the light **Q**. The output from the detector **S**, represents a measurement of the effect of the gap properties on the interference intensity.

$$S = P + Q + 2 \cdot \sqrt{P \cdot Q} \cdot \cos\left(\theta + \frac{2\pi n}{\lambda} \cdot 2L\right)$$

This expression includes the index of refraction **n**, of the gap material and the wavelength of light **λ**. The key is to extract a reliable and accurate estimate of **θ**, from the detector measurement of the power. One approach is to illuminate the gap sensor with four different lights each having a different wavelength, as we have it designed into the sensor interrogation system.

Optiphase carried out detailed mathematical derivations and analysis on how a successful quadrature measurement, calibration, demodulation and the phase angle measurement is achieved. The associated signal measurement and computation was subsequently implemented.

In the following section we show the successful integration and assembly of the interrogator system.

Component Integration & Chassis Assembly

The following components were integrated into a single Chassis.

- +5V Power Supply
- +/- 5V Power Supply
- SOA Pulser PCB with SOA
- SOA Temperature Controller
- Erbium Doped Fiber Amplifier (EDFA)
- Optical Circulator
- Dense Wave Division Multiplexer (DWDM)
- Timer CCT PCB
- The 4-Channel, Wideband Receiver PCB
- CB-68LPR Breakout PCB

The four wavelength laser source consists of a separate chassis which was shown previously.

The following aggregate components were tested and verified, and in some cases troubleshot and repaired.

- +/-5V Power Supplies
- SOA Pulser PCB with SOA and SOA Temperature Controller
- Erbium Doped Fiber Amplifier (EDFA)
- Optical Circulator
- Dense Wave Division Multiplexer (DWDM)
- The 4-Channel, Wideband Receiver PCB
- CB-68LPR Breakout PCB

Documentation was created for the following components:

- Chassis Power Wiring
- Chassis Signal Wiring
- Down-Hole Seismic Demo System Diagram

The completed assembly front panel is shown in Figure 26. The component layout inside chassis is shown and annotated in Figure 27.

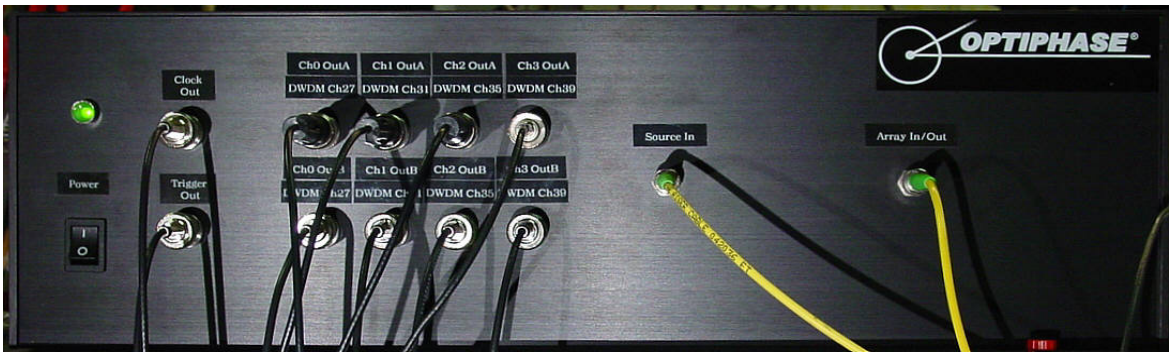

Figure 26. Interrogator Instrument Front Panel Layout.

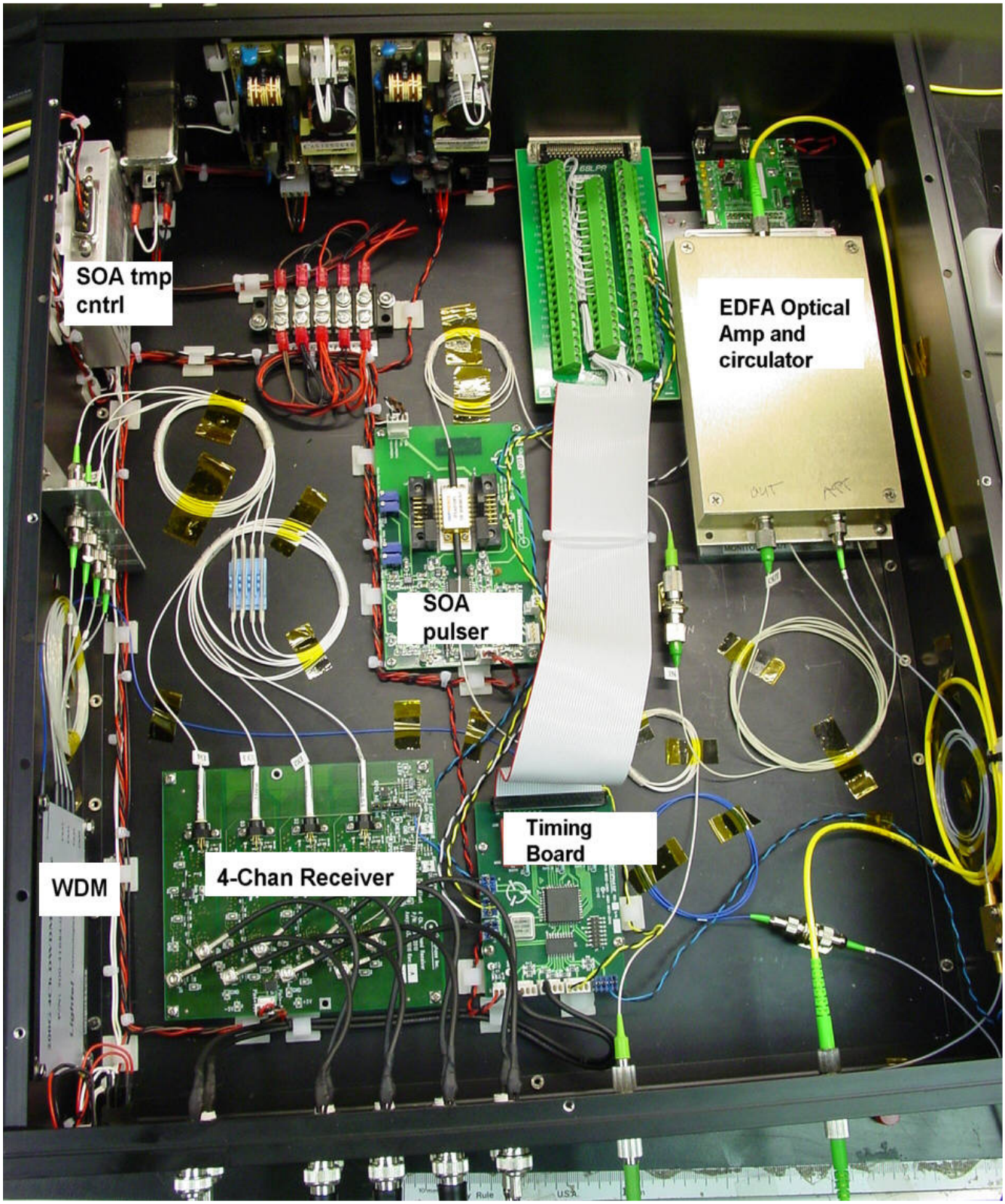

Figure 27. Interrogator Instrument Component Layout.

Control Software

Special purpose software was written to control the demonstation unit consisting of light sources, interrogator system and sensor mock-ups. The software is single stand-alone application that performs the following functions:

1. Controls the six Piezos with either sinusoidal signals or a user data file.
2. Controls the Opto-Electronic elements:
    - EDFA Current
    - Pulse Width
    - Pulse Rate
    - Trigger Delay
3. Performs the Acquisition of returned pulse signals.
4. Analyzes the return pulses and determines, for all six sensors:
    - Relative Displacement in Radians vs. Time
    - Unit Circle (X,Y plot)
    - FFT in Radians vs. Frequency
5. Allows the user to setup and save:
    - Piezo Drive Settings
    - Opto-Electronic Settings
    - Acquisition Settings
    - Analysis Settings
6. Displays Results:
    - Displacement results in radians for all six sensors
    - Unit Circle results for all six sensors (used for calibration)
    - FFT results for all six sensors
7. Data Archiving:
    - Data and Settings can be saved to file.
    - Saved Data and Settings can be opened from file and displayed

The Down Hole Seismic Demo Application is a LabView 8.2 application. This software runs under the National Instruments LabView 8.2 environment. In addition to requiring National Instruments' LabView to be installed, the application requires National Instruments NI-DAQ drivers to be installed for the PCI DAC Card (NI-6723) and UltraFast SPCM drivers to be installed for the PCI Digitizer Card (UF3131).

Integrated System Checkout

Various setup conditions were established during setup phase. Key conditions / issues resolved are itemized below:

- Optical gaps were set to 93.75 um based on swept laser, phase step approach.
- Calibration factors were determined for each of the two sources and entered. This was done by applying signals to each interferometer larger than 2 pi and measuring interferometric visibility range for each sensor. This procedure generated two sets of calibration files for each laser (broadband and four channel laser source).
- Timing delays were set up for the optical sensor simulator so that ADC strobes occurred simultaneous with pulse returns for each sensor. In this case a 10 MHz clock corresponding to 100 ns pulse width interrogation was used.
- Optical receiver were adjusted to accommodate input light levels such that output levels were matched to the ADC range.
- SOA pulse width was set to 100 nsec, drive current at maximum 250 mA.
- Optical Amplifier was configured for pump drive range between 100 and 250 mA which allows variations of the optical gain of the output pulse.
- Sample rate was set to 8 KHz.
- Data parameters were set for sample set size. Default set to 8192 points per set, such that FFTs conducted for data had nominally 1 Hz resolution bandwidth (good for noise analysis).
- FFT scalings were coordinated to provide RMS level data match to true displacement data.
- Optical receiver transimpedance amplifier circuits were observed to have 10-12 dB peaking ag 60 MHz. We had concerns that this peaking would cause a under-damped transient response to step type inputs (which is what TDM interrogation does). This was corrected by placing 0.4 pF parallel capacitors together with the 12Kohm transimpedance resistors. It was checked again and desired result was obtained. The bandwidth of receiver was reduced to approximately 45 to 50 MHz, and peaking as well as the resulting noise gain were eliminated. The magnitude of the transfer function showed that critical damping was accomplished.
- Software was fine-tuned during setup and various minor bugs were fixed.
- Sensor Simulation channels 1 and 2 suffered from broken leads to the piezo elements. They were left as is since no backup piezo elements were available and we were out of time and budget to resolve this issue. The four remaining working elements were more than sufficient for checkout and performance evaluations.

- Debug and repair to Piezo drive circuitry was carried out(Power conditioning capacitor failed, caused others to fail).

After the above test and adjustments were performed, the system became functional and operational. We were very pleased that the Optiphase team got such a complex system immediately working.

Software Operations

Several basic functions were tested with the software's operational interface. The display in Figure 29 shows the expected Lissajous patterns. In this case sensor #3 is driven at 100 Hz (13 rad P-P) causing the circular response as expected. The interface shows several pertinent parameters such as: "d" correction factors, which may be on-screen adjusted, piezo-electric drive levels, EDFA pump current settings, and selection taps for all the other sensors.

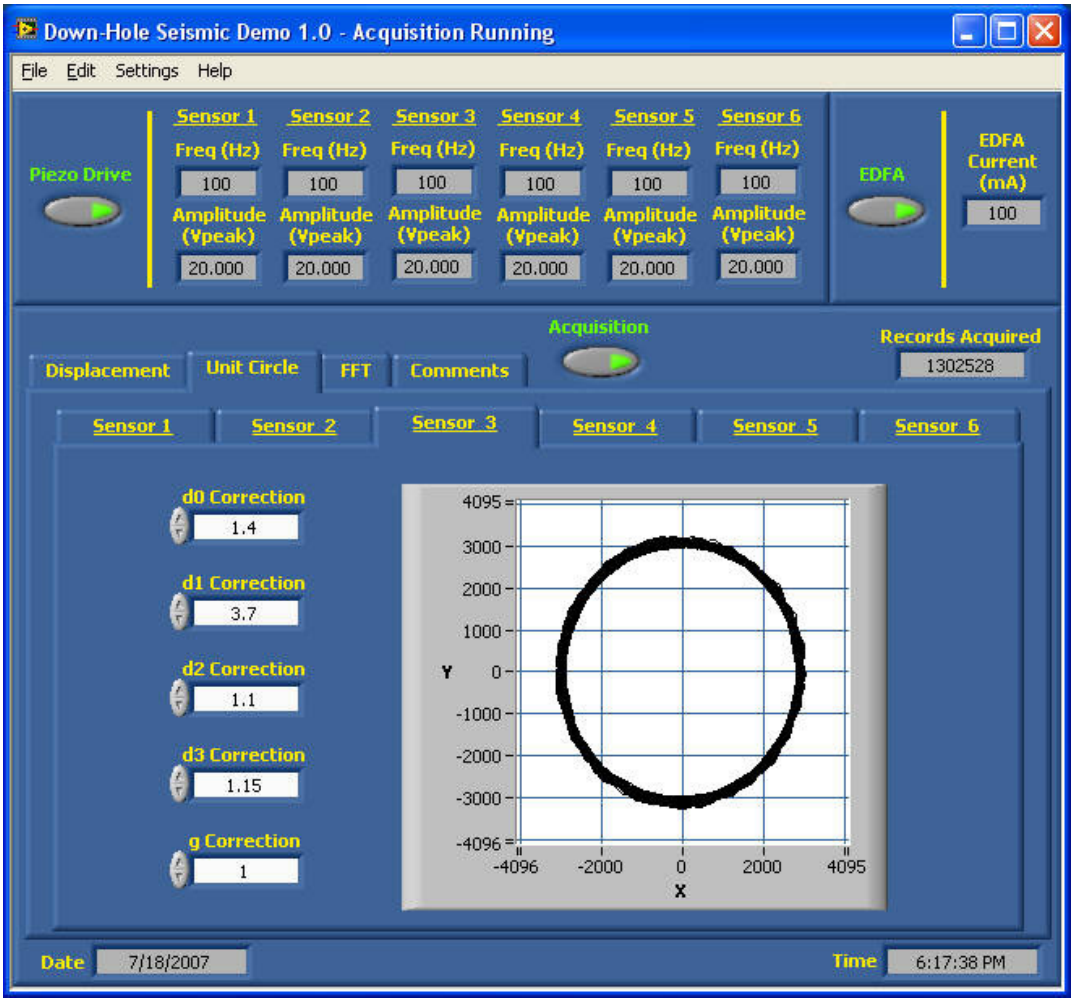

Figure 28: Lissajous pattern as recorded from sensor #3.

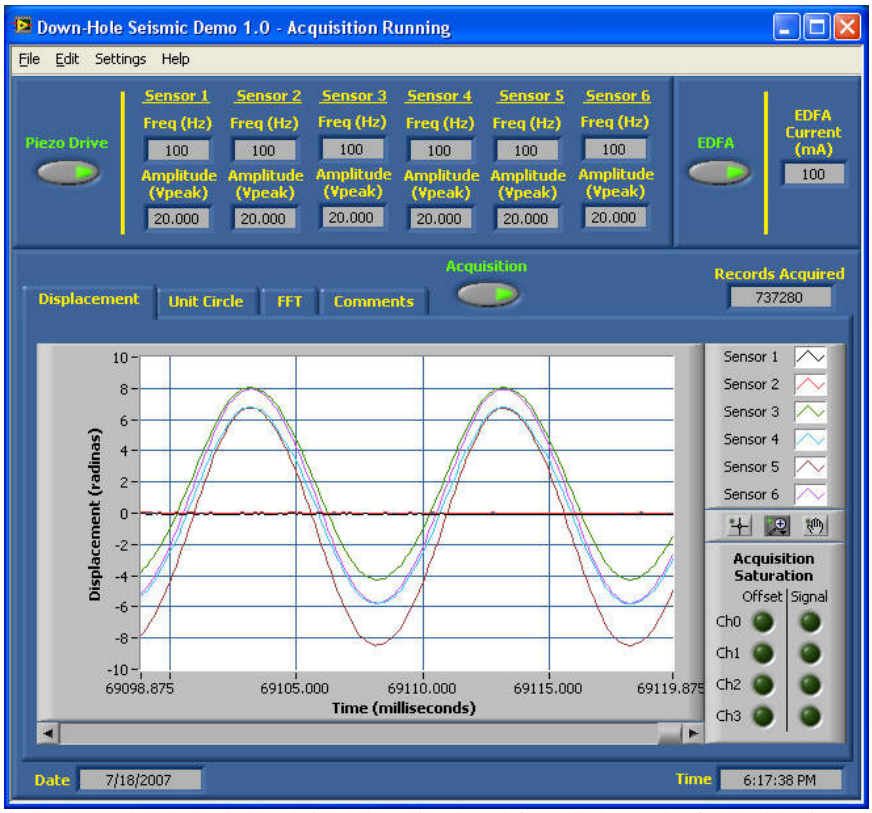

Figure 29: The demodulated time domain signal for all channels: four with sine wave signal, two with ambient noise.

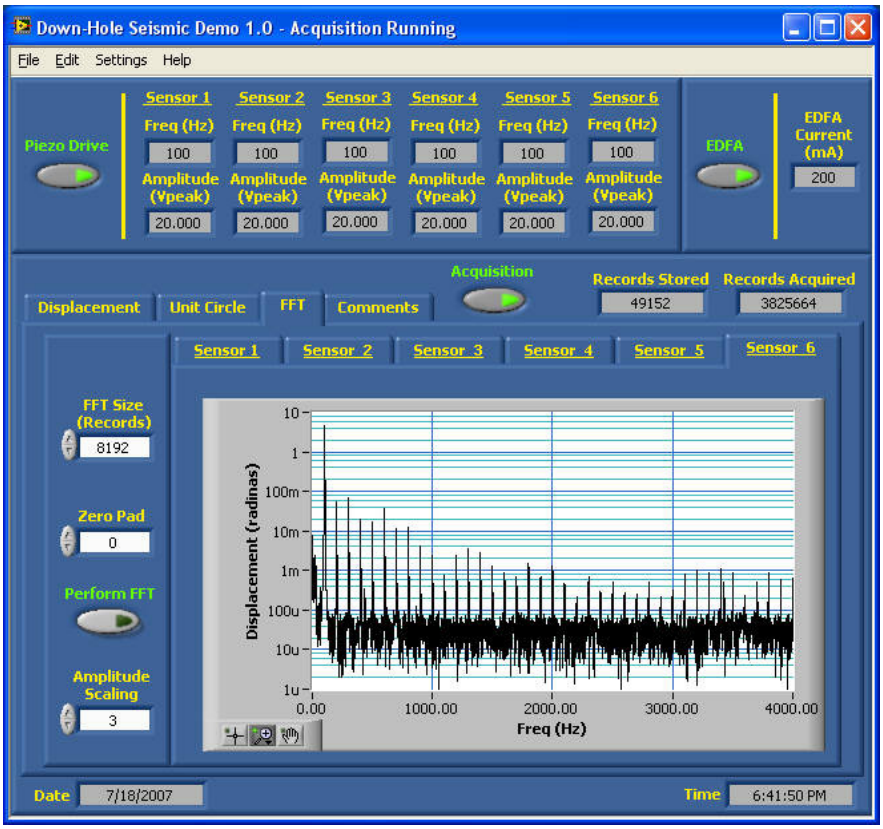

Figure 30: Fourier transform of sensor 6 recording the 100 Hz vibration.

Performance Evaluations

Using the complete integrated test bed, which included all components' performance tests were conducted with specific focus on noise, distortion and cross-talk. The details are summarized in this section.

Noise Tests

Noise measurements were carried with the selected set of sources: the broadband source and the Laser source. See previous sections on down-selecting different multi-wavelength source types. Evaluations of Fourier Transform were made on all channels. The results of the noise measurements were as follows:

Sensor	Noise Measured Micro-radians per root Hz Broadband Source	Noise Measured Micro-radians per root Hz Laser Source
1	250	**400**
2	300	**400**
3	175	**250**
4	200	**120**
5	225	40
6	225	30

The ideal performance would be in the range of 20 to 30 micro-radians per root Hz. The broadband source is above that ideal scenario. For the Laser source the sensors 5 and 6 exhibited nearly ideal performance.

Sensors 1-4 all were higher than expected for the Laser source. The cause for this was found to be related to the multiplex optics (see Fig 21). The 1X3 coupler components were providing some unwanted back-reflections causing a high return loss. These back reflections are coherent with the sensor returns and due to the relative large path mismatch of few to tens of meters. Thus, the phase noise is high as these lasers are highly coherent. In potential future activities the noise can be brought to nearly ideal levels by having these 1X3 components specified with a low return loss. These components are readily available at a slight cost premium.

The noise measurement for the broadband source was not expected. We expected to observe noise in the range of 50 urads/rt-Hz or less down to theoretical best of 20 urads/rt-Hz. If a broadband source is deployed, then some additional design tests will be required to determine the cause of the noise sources.

Based on noise measurement results, we selected the Laser source currently as the best candidate, which fulfilled the design requirements of the sensor interrogation system.

Distortion

Distortion was measured on all channels with active Piezo elements. The measurement was similar for all channels at -37 dB and was always dominated by third order harmonic terms. Most likely this was caused by the PZT elements and we expect that linearity of the interrogation process is much better than this level.

Crosstalk

In the interrogation system crosstalk can occur from optical bleed over from one channel to an immediate adjacent neighbor. For this test system, we employed a standard measurement technique and measured crosstalk by driving one channel and looking at neighboring channels. In this case one channel was driven in turn with 100 Hz RMS 4.5 radians, while all other channels were not driven.

In most cases, crosstalk was unobservable, since it was below the noise level. A summary of the crosstalk measured:

CHAN 3 On	Channel 2 Xtalk =	< - 76 dB	Chan 4 Xtalk	- 64 dB
CHAN 4 On	Channel 3 Xtalk =	< - 76 dB	Chan 5 Xtalk	- 76 dB
CHAN 5 On	Channel 4 Xtalk =	< - 76 dB	Chan 6 Xtalk	- 67 dB
CHAN 6 On	Channel 5 Xtalk =	< - 73 dB	NA	

We suspect all crosstalk above -70 dB was really related to mechanical pickup rather than optical due to the close proximity of the channel simulators. Thus, the crosstalk, as measured here, was quite good and suitable for the sensing application.

Interrogator System Conclusions

The overall effort relating to the development of an interrogation approach for MEMS seismic sensors which are TDM multiplexed was considered to be successful. The demonstration system showed it to be functionally viable and key criteria for performance showed the capability for high performance.

Minor issues relating to noise performance and errors in the telemetry optics can be easily addressed when implementing a commercial system. We originally thought that a broadband source would provide better noise performance. However, our tests showed that excess noise existed in that case. Thus, if a broadband source is to be used, this excess noise needs to be investigated further. Currently the Laser source provides superior noise performance throughout the interrogation process.

Conclusions

During the course of this project we designed, prototyped and tested various components of a robust multi-component sensor that combines both Fiber Optic and MEMS technology for use in a borehole seismic array. Design, packaging, material selection and integration of the multi-component sensors and deployment system targeted a maximum operating temperature of 350-400 deg F and a maximum external pressure of 15000-25000 psi. This project tried to leverage existing pieces of deployment technology as well as MEMS and fiber-optic technology and combine them in an optimal way.

While this project was planned to be conducted in two phases, DOE funding restrictions allowed us only to work up to the first phase and thus, complete only the sensor design and interrogator testing without going into manufacturing of the MEMS sensor devices. For the contract award period Paulsson Geophysical and its main subcontractor Optiphase worked on a wide range of activities from detailing specifications, designing and testing subsystems to interfacing with and selection of potential manufacturing subcontractors.

Originally PGSI had planned to work with subcontractor Umachines Inc., but both parties could not come to an agreement relating the future use of intellectual property. After extended discussion Umachines retracted and Paulsson Geophysical, after having looked into several alternatives, proceeded subcontracting with Optiphase Inc. as the main subcontractor to support PGSI in development of the MEMS sensor and interrogation package as well as with management of external project details and other potential subcontractors.

By year end of 2006 two events caused a change in focus of the project. One was the inability to secure a manufacturing contract with David Instruments as a MEMS manufacturer and integrator for construction of the MEMS sensors. The other was that Department of Energy funds for the second phase of the project became unavailable due to budget cuts. At that time with concurrence of the DOE project manager, the project was refocused to complete the basic design of the MEMS sensor without going into manufacturing; and to design, implement and test a prototype of the time and wavelength domain multiplexed fiber-optic gapped sensor interrogator by July 2007. Thus, we were able to complete some of the advanced tasks that were originally scheduled for the second phase.

This worked out well, since we could accomplish many of the tasks that were slated for the later phase of the project. These tasks mainly concerned the interrogator system design, prototyping of sensor drop-in and interrogation system components, as well as functionality tests of the assembled interrogator prototype system in the laboratory. We performed work described in the statement of project objectives task 1-5, 9p, 15-19, 21 and 22. These tasks relate to design, prototyping and testing of sensors and the interrogation system. Instead of the prototyped MEMS sensors, drop-in proxies were used and work continued using these specific proxy devices. These omitted tasks were

mainly re-design/re-test/re-manufacturing iterations to optimize the sensor performance in practice.

Thus, by the end of project we were able to successfully complete the following major tasks:

- specifications for a gap based fiber optic sensor
- selection of a practical gap-based sensor device design
- specification and design of sensor packaging
- test and selection of appropriate light sources
- design of an advanced interrogation system
- test of component for the interrogation system
- construction of a table top prototype assembly of the time and wavelength domain multiplexed interrogator system
- design of control software
- design of the recording interfaces
- implementation of control software for the table top prototype
- completion of multi-channel performance measurements

Many design, manufacturing and technical issues were encountered and have been solved in the course of this project. This report provides a summary for the contracted activities during the project period from October 2004 through July 2007.

References

Bass, M. and Van Stryland, E.W., 2002, Fiber Optics Handbook, McGraw-Hill, OSA.
Friedman, E, and Miller, J.L, 2003, Photonics Rule of Thumb, McGraw-Hill, SPIE Press.
Goff, D.R., 2002, Fiber Optic Reference Guide, 3rd Ed., Focal Press, Elsevier Science.
W. Young. *Roak's Formulas for Stress & Strain*. McGraw-Hill Inc., sixth edition, 1989.
Marc J. Madou, Fundamental of Microfabrication, CRC press, 2002.
"Hermetic Packaging: a neglected 'Holy Grail'?" http://www.resonetics.com/PDF/Light-wave.pdf
http://www.optiforms.com/
http://www.ioffe.rssi.ru/SVA/NSM/Semicond/Si/

Cooper, E.B. et al, 2000, Appl. Phys. Lett. 76, 3316.

Malki, A. et al, 1995, Appl. Opt. 34, 8014.

Jeunhomme, Single Mode Fiber Optics, Marcel Dekker, p. 100.

T. Hsu, MEMS and Microsystems: Design and Manufacture, McGraw-Hill.

http://www.ofsoptics.com/
http://www.specialtyphotonics.com/

National Energy Technology Laboratory

626 Cochrans Mill Road
.O. Box 10940
Pittsburgh, PA 15236-0940

3610 Collins Ferry Road
P.O. Box 880
Morgantown, WV 26507-0880

One West Third Street, Suite 1400
Tulsa, OK 74103-3519

1450 Queen Avenue SW
Albany, OR 97321-2198

539 Duckering Bldg./UAF Campus
P.O. Box 750172
Fairbanks, AK 99775-0172

Visit the NETL website at:
www.netl.doe.gov

Customer Service:
1-800-553-7681